Title

The NASA Twins Study: A multidimensional analysis of a year-long human spaceflight

Journal

Science, 364(6436)

ISSN

0036-8075

Authors

Garrett-Bakelman, Francine E
Darshi, Manjula
Green, Stefan J
et al.

Publication Date

2019-04-12

DOI

10.1126/science.aau8650

Peer reviewed

HHS Public Access

Author manuscript

Science. Author manuscript; available in PMC 2020 October 22.

Published in final edited form as:

Science. 2019 April 12; 364(6436): . doi:10.1126/science.aau8650.

The NASA Twins Study: A multidimensional analysis of a year-long human spaceflight

A full list of authors and affiliations appears at the end of the article.

Abstract

INTRODUCTION: To date, 559 humans have been flown into space, but long-duration (>300 days) missions are rare (n = 8 total). Long-duration missions that will take humans to Mars and beyond are planned by public and private entities for the 2020s and 2030s; therefore, comprehensive studies are needed now to assess the impact of long-duration spaceflight on the human body, brain, and overall physiology. The space environment is made harsh and challenging by multiple factors, including confinement, isolation, and exposure to environmental stressors such as microgravity, radiation, and noise. The selection of one of a pair of monozygotic (identical) twin astronauts for NASA's first 1-year mission enabled us to compare the impact of the spaceflight environment on one twin to the simultaneous impact of the Earth environment on a genetically matched subject.

RATIONALE: The known impacts of the spaceflight environment on human health and performance, physiology, and cellular and molecular processes are numerous and include bone density loss, effects on cognitive performance, microbial shifts, and alterations in gene regulation. However, previous studies collected very limited data, did not integrate simultaneous effects on multiple systems and data types in the same subject, or were restricted to 6-month missions. Measurement of the same variables in an astronaut on a year-long mission and in his Earth-bound twin indicated the biological measures that might be used to determine the effects of spaceflight. Presented here is an integrated longitudinal, multidimensional description of the effects of a 340-day mission onboard the International Space Station.

[§§]Corresponding author. jbcharle@gmail.com (J.B.C); craig.e.kundrot@nasa.gov (C.E.K.); graham_b_scott@yahoo.com (G.B.I.S.); susan.bailey@colostate.edu (S.M.B.); basner@pennmedicine.upenn.edu (M.B.); afeinberg@jhu.edu (A.P.F.); stuart.lee-1@nasa.gov (S.M.C.L.); chm2042@med.cornell.edu (C.E.M.); mignot@stanford.edu (E.M.); bkrana@ucsd.edu (B.K.R.); scott.m.smith@nasa.gov (S.M.S.); mpsnyder@stanford.edu (M.P.S.); fturek@northwestern.edu (F.W.T.).

[*]These authors contributed equally to this work.

[†]Present address: Providence Portland Medical Center, Portland, OR, USA.

[‡]Present address: HudsonAlpha Institute for Biotechnology, Huntsville, AL, USA.

[§]Present address: Brown University, Providence, RI, USA.

[¶]Present address: Augusta University, Augusta, GA, USA.

[#]Present address: IUBH International University of Applied Sciences, Bad Reichenhall, Germany.

[**]Present address: Mayo Clinic, Rochester, MN, USA.

[††]Present address: Nara Medical University, Nara, Japan.

[‡‡]Present address: Institute for Advanced Biosciences, Keio University, Tokyo, Japan.

SUPPLEMENTARY MATERIALS www.sciencemag.org/content/364/6436/eaau8650/suppl/DC1

Materials and Methods

Figs. S1 to S15

Tables S1 to S11

References (85–156)

RESULTS: Physiological, telomeric, transcriptomic, epigenetic, proteomic, metabolomic, immune, microbiomic, cardiovascular, vision-related, and cognitive data were collected over 25 months. Some biological functions were not significantly affected by spaceflight, including the immune response (T cell receptor repertoire) to the first test of a vaccination in flight. However, significant changes in multiple data types were observed in association with the spaceflight period; the majority of these eventually returned to a preflight state within the time period of the study. These included changes in telomere length, gene regulation measured in both epigenetic and transcriptional data, gut microbiome composition, body weight, carotid artery dimensions, subfoveal choroidal thickness and peripapillary total retinal thickness, and serum metabolites. In addition, some factors were significantly affected by the stress of returning to Earth, including inflammation cytokines and immune response gene networks, as well as cognitive performance. For a few measures, persistent changes were observed even after 6 months on Earth, including some genes' expression levels, increased DNA damage from chromosomal inversions, increased numbers of short telomeres, and attenuated cognitive function.

CONCLUSION: Given that the majority of the biological and human health variables remained stable, or returned to baseline, after a 340-day space mission, these data suggest that human health can be mostly sustained over this duration of spaceflight. The persistence of the molecular changes (e.g., gene expression) and the extrapolation of the identified risk factors for longer missions (>1 year) remain estimates and should be demonstrated with these measures in future astronauts. Finally, changes described in this study highlight pathways and mechanisms that may be vulnerable to spaceflight and may require safeguards for longer space missions; thus, they serve as a guide for targeted countermeasures or monitoring during future missions.

Abstract

To understand the health impact of long-duration spaceflight, one identical twin astronaut was monitored before, during, and after a 1-year mission onboard the International Space Station; his twin served as a genetically matched ground control. Longitudinal assessments identified spaceflight-specific changes, including decreased body mass, telomere elongation, genome instability, carotid artery distension and increased intima-media thickness, altered ocular structure, transcriptional and metabolic changes, DNA methylation changes in immune and oxidative stress–related pathways, gastrointestinal microbiota alterations, and some cognitive decline postflight. Although average telomere length, global gene expression, and microbiome changes returned to near preflight levels within 6 months after return to Earth, increased numbers of short telomeres were observed and expression of some genes was still disrupted. These multiomic, molecular, physiological, and behavioral datasets provide a valuable roadmap of the putative health risks for future human spaceflight.

Graphical Abstract

Multidimensional, longitudinal assays of the NASA Twins Study. (Left and middle) Genetically identical twin subjects (ground and flight) were characterized across 10 generalized biomedical modalities before (preflight), during (inflight), and after flight (postflight) for a total of 25 months (circles indicate time points at which data were collected). (Right) Data were integrated to guide biomedical metrics across various "-omes" for future missions (concentric circles indicate, from inner to outer, cytokines, proteome, transcriptome, and methylome).

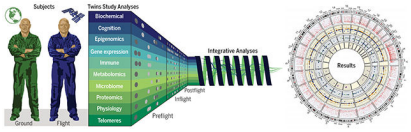

Hundreds of humans have flown in space since 1961, providing insight into the effects of environmental factors—including weightlessness, unloading, and radiation exposure—on the physiological responses of the human body and their functional consequences. Human physiological adaptation to short-duration (<1 month) and longer-duration (>4 months) spaceflight have been described, particularly for the cardiovascular, musculoskeletal, and sensorimotor systems (1). Some changes, such as headward fluid shift, are rapid and reach a new steady state relatively quickly (within days). By contrast, the nature of change in cardiovascular and muscular traits during longer missions is more pronounced, and their rate of return to baseline after spaceflight is prolonged (2). The headward fluid shift occurs immediately upon entry into weightlessness (3), resulting in a decrease in plasma and blood volume during the first few days of a mission (4) that plateaus in the first 2 weeks of flight. However, the decrease in plasma volume and red blood cells is not significantly different for short- or long-duration missions (5). Conversely, cardiovascular adaptations (e.g., left ventricular mass increase) and resulting downstream outcomes (e.g., orthostatic tolerance and maximal oxygen consumption losses) become more pronounced with longer-duration missions (5–8). Similarly, loss of muscle mass and strength are greater after longer-duration spaceflight (9–11). The adverse effects of these adaptations are especially clear upon return to Earth. Regular vigorous exercise, combined with adequate nutrition during spaceflight, mitigate some of the spaceflight-induced muscle (9, 12) and bone loss (13) that occur during both short- and long-duration missions. However, recent evidence suggests that long-duration missions on the International Space Station (ISS) have resulted in some astronauts developing ocular changes, including optic disc edema and choroidal folds (14, 15), termed spaceflight-associated neuro-ocular syndrome (SANS) (16). The incidence and severity of ocular symptoms varies, and the exact mechanism for the development of SANS is not well understood, which has limited NASA’s ability to develop an effective countermeasure.

Although our understanding of the physiological and functional consequences of 4- to 6-month missions has increased greatly over the 18 years of continuous human presence on the ISS, there is almost no experience with spaceflight length greater than 6 months. Future missions, however, could be as long as 3 years, including transit to and from Mars and possible exploration of the planet, yet only four individuals have participated in spaceflight missions lasting 1 year or more. Moreover, investigations have not consistently implemented an integrated, cross-discipline study design or utilized multiomic approaches to biospecimen analyses. Thus, we have limited knowledge of the full range of the interactions of molecular, physiological, and cognitive dynamics that occur during long-duration spaceflight. Given the increasing number of vehicles providing access to spaceflight (17) and proposed missions to Mars, studies are needed to better understand the impact of prolonged spaceflight on human biology and health. Genetic, immune system, and metabolic functions are of particular concern given exposure to space radiations, restricted diet, reduced physical work requirements, disrupted circadian rhythms, and weightlessness. Importantly, longitudinal

measures of biomarkers (such as genomic, epigenomic, biochemical, and physiological alterations) can provide critical metrics for astronaut health that could aid in assessment of increased risks and guide potential personalized interventions.

The NASA Twins Study investigators leveraged the opportunity to study identical twin astronauts, one in space and one on Earth. Data were generated from specimens collected and test protocols administered over 25 months, spanning time points before (preflight), during (inflight), and after (postflight) spaceflight with an integrated sampling scheme (Fig. 1A), including a wide variety of biological samples as well as cognitive and physiological measures (Fig. 1A and table S1). Our study also provides an example of inflight data and sample collection strategies used to generate a comprehensive, longitudinal, molecular, physiological, and cognitive profile, providing a scientific framework and baseline data for future studies. It is important to note that with a single test subject in the spaceflight environment for this particular set of measures, it is impossible to attribute causality to spaceflight versus a coincidental event. Therefore, our study should be considered as hypothesis-generating and framework-defining and must be complemented in the future by studies of additional astronauts.

Results

A pair of male monozygotic twins were studied, one of whom spent 340 days aboard the ISS (flight subject; TW), while his identical twin remained on Earth (ground subject; HR). The subjects were 50 years of age at the time of study initiation and had accumulated different amounts of prior spaceflight exposure (Table 1). TW had, over the course of 12 years, a total of 180 days in space before the 1-year mission; there was a 4-year gap from the end of the previous long-duration mission until the start of this study. By contrast, HR had a total of 54 days in space and, at the time of this study, had not flown in space for almost 4 years.

Collected samples ($n = 317$) from both subjects throughout the duration of the study included stool, urine, and whole blood, which was also separated into peripheral blood mononuclear cells (PBMCs), sorted immune cells, and plasma. These samples were assayed for epigenomic, metabolomic, transcriptomic, proteomic, molecular, and microbiome changes (Fig. 1A and table S1). Additionally, subjects participated in physiological and cognitive tests in the laboratory during preflight and postflight ground-based testing and onboard the ISS (inflight).

Extensive multisystem changes occur in spaceflight

Data were generated from fresh (FR) and ambient return (AR) whole blood or PBMCs that were either directly processed and fractionated into subpopulations (T cells: CD4 and CD8; B cells: CD19; and lymphocyte depleted: LD) (fig. S1) or processed directly from frozen PBMCs. For fractionated subpopulations, the inflight collections were confounded by ambient return (AR specimens were collected on the ISS and returned to Earth via Soyuz capsule at room temperature). To simulate this effect, independent samples were generated to mimic FR and AR sample collection conditions and used for correction. Unsupervised analysis of gene expression profiles segregated TW's inflight from preflight and postflight samples, as well as from HR specimens, for all cell populations examined (fig. S2, A to E).

Similar expression changes were observed for all cell types assessed (Fig. 1B). Differentially expressed genes (DEGs, DESeq2 multivariate negative binomial model, $q < 0.01$) were identified across all samples and cell types ($n = 9317$) with HR as the control and a particular focus on the differences that persisted postflight. In the LD cell population, of the 481 DEGs found inflight, compared with preflight, there were 112 (23.2%) that remained differentially expressed postflight (Fig. 1B and table S2). Across all sorted cell types, only 811 of the inflight DEGs remained disrupted postflight. Concomitant with an overall shift in mitochondrial RNA (mtRNA) levels (see below), far more DEGs ($n = 8564$, DESeq2 multivariate negative binomial model, $q < 0.01$) were observed in the 6- to 12-month inflight period compared with HR than in the 0- to 6-month inflight period ($n = 1447$) in PBMCs. This large (6×) shift in overall gene regulation upon exposure in TW to a year-long spaceflight suggests that overall gene regulation may be more affected by longer-duration spaceflight.

To assess physiological and immune signaling changes, the metabolome, proteome, and cytokine complement were measured using mass spectrometry and antibody-based methods. Targeted and untargeted metabolomics and proteomics were performed on plasma and urine samples, whereas cytokine profiling was performed only on plasma samples (fig. S3 and table S1). Untargeted analysis was focused on a high-confidence set of 719 metabolites (out of 4162 metabolic features) identified in plasma using a broad-spectrum liquid chromatography–mass spectrometry (LC-MS) metabolomics platform (18). Linear models demonstrate significant differences [false discovery rate (FDR) < 0.05] in the abundance of 245 metabolites among pre-, in-, and postflight samples between TW and HR, including those specific to the earlier or later halves of the flight period as well as those associated with time spent on the ISS (Fig. 1C and table S3). Additionally, 39 metabolites were significantly different (FDR < 0.05) between TW and HR at baseline (table S3). Metabolites indicative of genotoxic stress, inflammation, and altered amino acid metabolism were increased in TW inflight (table S3). Targeted metabolomic analysis using gas chromatography–tandem mass spectrometry (GC-MS/MS) was performed in plasma and urine to quantify metabolites involved in the tricarboxylic acid (TCA) cycle, glycolysis, and amino acid, fatty acid, ketone body, and pyrimidine metabolism. Of the 81 targeted metabolites, 60 and 66 metabolites were detected in plasma and urine, respectively (table S3). No significant changes were observed in plasma metabolites, but 32 urinary metabolites were significantly altered inflight for TW [FDR: $P < 0.05$, analysis of variance (ANOVA)]. To assess the epigenetic contribution to the changes observed, whole-genome bisulfite sequencing (WGBS) was performed on a subset of CD4 and CD8 samples from each subject. Global DNA methylation changes in TW were within the range of variation seen in HR throughout the study. However, ontology analysis of genes ranked on the basis of epigenetic discordance, as quantified by average promoter Jensen-Shannon distance (JSD) between samples, revealed distinct pathways enriched in TW when comparing preflight with inflight samples (Fig. 1D and tables S4 and S5). For example, in CD8 cells, enrichment in regulation of neutrophil activation or granulation was observed in TW [$q < 0.01$, hypergeometric test (HGT)], but not in HR (Fig. 1D). Similarly, in CD4 cells, enrichment in platelet aggregation ($q = 0.0002$, HGT) was observed only in TW.

To identify complex changes spanning diverse analyte classes that occur over time, the different data types were combined and scaled, and *c*-means clustering analysis was performed. Although this analysis (Fig. 1E) revealed that physiological levels for a large number of analytes were unaffected by spaceflight (Fig. 1E; clusters 1 and 2), several notable patterns were identified. These included a cluster of features, including cognitive performance, that for TW increased inflight and declined sharply upon return before reaching baseline (Fig. 1E, cluster 3; and Fig. 1F); this cluster was enriched for analytes involved in central carbon metabolism [$q < 0.0002$; integrated molecular pathway level analysis (IMPaLA) combined pathway analysis, Fisher's method]. Integrating gene expression changes with the other analytes revealed additional complex biochemical trajectories; for example, gene expression changes associated with neutrophil regulation were enriched ($q < 1 \times 10^{-12}$; IMPaLA combined pathway analysis, Fisher's method) in cluster 25 (fig. S5), illustrating an increase very early inflight followed by a steady decline, until increasing again postflight.

Telomeres lengthened during spaceflight

Telomeres are repetitive features of chromosomal termini essential for maintaining genomic integrity; they protect physical DNA ends from degradation and prevent them from triggering inappropriate DNA damage responses (DDRs). Telomere length shortens with cell division and thus with age, as well as with a variety of lifestyle factors, such as stress, and environmental exposures, including air pollution and radiation. Here, average telomere length was evaluated pre-, in-, and postflight (DNA; PBMCs) using quantitative real-time polymerase chain reaction (qRT-PCR) (19, 20). Consistent with a strong genetic component (21), HR and TW had similar telomere lengths at baseline (preflight $P = 0.942$; one-way ANOVA), and telomere lengths for HR remained relatively stable for the duration of the study (Fig. 2A). Most notable was a significant increase in telomere length during flight for TW (14.5%), as compared with his preflight and postflight measures as well as with those of HR ($P = 0.048$, 0.0003, and 0.0073, respectively; one-way ANOVA). TW's increased telomere length was observed at all inflight time points assessed [flight day (FD) 14 to FD334; fig. S6A], as well as in sorted CD4, CD8, and LD cells, but not in CD19 cells (Fig. 2B and fig. S6B). These results are consistent with recently reported cell type-specific responses to factors that contribute to telomere length regulation (22). Notably, telomere length shortened rapidly upon TW's return to Earth, within ~48 hours [FD340 ambient return to R+0 (R+ days post return); fig. S6B] and stabilized to near preflight averages within months.

Additionally, metaphase chromosomes were prepared from pre-, in-, and postflight samples (stimulated T cells; ambient whole blood), and thousands of individual telomeres were evaluated with telomere fluorescence in situ hybridization (Telo-FISH) (23, 24), an independent measure that showed the same trends observed with qRT-PCR (fig. S6C). Importantly, Telo-FISH cell-by-cell analyses also enabled generation of telomere length distributions that confirmed HR's relatively stable telomere lengths throughout the study (Fig. 2C and fig. S6D). Consistent with TW's increased average telomere length during spaceflight, temporal shifts toward increased numbers of longer telomeres and concurrent decreases in the numbers of shorter telomeres were also observed (fig. S6D); for example,

there was a significant shift in TW's inflight (FD259) telomere length distribution as compared to his preflight (L–162; L– days before launch) distribution ($P < 2.2 \times 10^{-16}$; Mann-Whitney U test) (Fig. 2D). After returning to Earth (R+190), TW's telomere length distribution shifted back toward increased numbers of shorter telomeres, more closely resembling his preflight distribution. However, an increased number of signal-free chromosome ends, indicative of complete loss and/or critically short telomeres (i.e., below our level of resolution), was also apparent (Fig. 2D). Spaceflight-specific shifts in telomere length dynamics were also supported by gene expression results, in that when inflight, TW'sdown-regulated DEGs were significantly enriched in packaging-of-telomere ends and telomere-maintenance pathways, in both CD4 and CD8 cells [gene set enrichment analysis (GSEA), all $q \leq 0.001$] (table S2). Similarly, changes in DNA methylation of the gene promoter for *TERT*, which encodes the regulatory subunit of telomerase, were observed when comparing preflight with the late inflight time point in both CD4 and CD8 T cells (JSD rank 248 and 32, respectively); by contrast, for HR, *TERT* was not highly ranked (428 or greater) (table S5).

Telomerase is the reverse transcriptase capable of de novo addition of species-specific telomeric repeats onto the ends of newly replicated chromosomes (25). Telomerase activity was evaluated pre-, in-, and postflight (PBMCs, ambient) with the qRT-PCR telomeric repeat amplification protocol (TRAP) (24, 26). In general, TW had lower levels of telomerase activity than HR throughout the study, whereas levels for the two individuals were similar preflight and postflight (fig. S6E). Unfortunately, telomerase activity was lost in all inflight samples collected onboard the ISS. Given the sensitivity of enzymatic activity to sample handling conditions, we speculated that unavoidable transit time and/or temperatures associated with ambient return (via Soyuz) destroyed telomerase activity. To test this hypothesis, we compared ground control samples that had been in transit ≤24 hours with those that had been in transit ≥48 hours, mimicking the transit time from the ISS to Johnson Space Center. Loss of telomerase activity was observed in all blood samples experiencing transit times ≥48 hours ($P = 0.002$; Student's t test); however, telomere length and DNA integrity were unaffected (fig. S6, F to H).

DNA damage responses during spaceflight

Chromosome aberrations were analyzed in the same samples as above to evaluate potential telomere-related instability (e.g., fusions) as well as to assess DDRs to ionizing radiation (IR) exposure during spaceflight (27), specifically galactic cosmic ray (GCR)–induced cytogenetic damage, as has been done previously in blood lymphocytes of astronauts (28). Here, high-resolution directional genomic hybridization (dGH) paints (29) for chromosomes 1, 2, and 3 were used to enable simultaneous detection of interchromosomal translocations and intrachromosomal inversions (Fig. 2E). Baseline frequencies of these structural variants were similar for the two subjects, with inversions being more frequent than translocations (Fig. 2F). TW's inversion frequencies increased at a greater rate than translocations, consistent with inflight IR exposure, particularly to high linear energy transfer (LET) space radiation (30, 31). Indeed, a physical dosimeter dose of 76.18 milligrays and an effective dose of 146.34 millisieverts were recorded by NASA. Also consistent with IR exposure, genes whose expression was altered inflight were significantly enriched in pathways related

to DNA damage responses in LD, CD4, CD8, and PBMCs [generalized linear model (GLM), all $q \leq 0.002$; table S2]. Furthermore, TW's inversion frequencies continued to rise postflight, indicative of instability and possibly reflective of IR-induced DNA damage to stem cell compartments. Although TW's translocation frequencies were variable, translocations were also increased inflight and postflight compared with preflight, additional evidence of inflight radiation exposure and the persistence of GCR-induced cytogenetic damage (32).

DNA methylation patterning during spaceflight

We also examined DNA methylation in FR and AR specimens (Fig. 1A and table S1). Genome-wide DNA methylation levels were measured in CD4 and CD8 lymphocytes isolated from both subjects at four time points throughout the study: one preflight, two inflight (early and late), and one postflight. Principal components analysis (PCA) revealed a distinction in global DNA methylation between the two cell types and between subjects for the CD4 samples (Fig. 3A). Moreover, TW's inflight samples were distinct from preflight and postflight samples for both cell types. Subtle differences in both genome-wide mean methylation levels (MML) and normalized methylation entropy (NME; a measure of methylation stochasticity) were detected inflight for TW, which returned to baseline postflight (Fig. 3B). Although for HR, the direction of these changes was consistent in CD4 and CD8 cells, it was reversed for TW, with a decrease in MML at FD259 for CD4 cells and an increase in CD8 cells. Although MML and NME are not necessarily predictive of one another (33), an inverse relationship between genome-wide medians of MML and NME is evident across all samples. Importantly, the magnitude of changes in both MML and NME was greater for HR and did not fully return to baseline. These data indicate that genome-wide DNA methylation changes detected in CD4 and CD8 cells from TW were within the range of variation seen in HR.

These results identify only limited epigenetic discordance in global methylation and entropy levels. Therefore, we quantified both global and local epigenetic discordances between samples by calculating JSDs among all relevant pairwise comparisons within a cell type. Peaks of JSD indicate observable changes in the probability distributions of methylation levels within genomic regions, even if changes in mean methylation levels are small. Genome-wide JSD analysis revealed only subtle changes when comparing preflight with inflight or postflight samples within a subject (Fig. 3C). By contrast, we observed greater JSD changes in comparisons between subjects, particularly in CD4 cells (fig. S7A), consistent with our observation of higher MML and NME changes in that cell type (Fig. 3B). Similar to the results associated with methylation level and entropy, the magnitude of JSD changes was slightly greater for HR than for TW, again indicating that global methylation changes in TW were within the range observed for HR.

Although the observed genome-wide changes were minimal, we hypothesized that local changes at promoters of genes involved in environmental adaptation could be particularly affected in TW during flight. We therefore ranked genes according to their epigenetic discordance, as quantified by the JSD, and used these ranked lists for gene ontology (GO) enrichment analysis (table S4). When comparing inflight with preflight samples from TW,

we observed enrichments for genes involved in the response to platelet-derived growth factor (PDGF) and T cell differentiation and activation pathways in both CD4 and CD8 cells (Fig. 3D). Genes involved in platelet aggregation ($q = 0.028$, HGT), regulation of ossification ($q = 0.009$, HGT), and cellular response to ultraviolet-B (UV-B) ($q = 0.039$, HGT) were also enriched in these comparisons, specifically in CD4 cells. By contrast, analysis of CD8 cells revealed enrichment in genes involved in the somatostatin signaling pathway ($q = 0.016$, HGT) and positive regulation of superoxide anion generation ($q = 0.016$, HGT). Importantly, for all time point comparisons, the most enriched GO terms for TW preflight versus inflight were not enriched in HR (Fig. 1D).

Immune response and inflammation during spaceflight

Differential gene expression analysis indicated that many immune-related pathways were significantly changed inflight across all cell types (GLM, $q < 0.001$), including the adaptive immune system, innate immune response, and natural killer cell-mediated immunity (table S2). Additionally, DNA methylation analysis revealed epigenetic discordance (indicated by JSD peaks) for TW in the promoters of *NOTCH3*, a well-known regulator of T cell differentiation (34), and *SLC1A5/ASCT2*, which promotes T cell activation (35), between preflight (L–162) and inflight samples (FD259 for *NOTCH3* and FD76 for *SLC1A5*) in CD4 and CD8 cells, respectively (Fig. 3E). This epigenetic discordance was associated with a peak of increased promoter methylation (from 10.7 to 20.2%) and entropy (from 41.4 to 71.3%) during flight and was observed in TW, but not in HR nor between HR and TW in preflight samples (fig. S7, B and C), and for *SLC1A5*, was associated with differential expression (down-regulation) (table S2).

To further evaluate T cell and immune functionality in spaceflight, we assessed cytokine data for inflammation signatures. Although none of the cytokines assayed were significantly different at baseline between TW and HR, 50 of the 62 cytokines assayed were differentially abundant between pre-, in-, and postflight in TW. We observed three notable signatures of inflammation. The first signature was composed of cytokines whose levels rose in TW's plasma in the days after return and continued to be increased 6 months after return. These return-associated cytokines included CSF2 (GM-CSF), HGF, IL10, IL17A, IL18, LEP (leptin), CD40LG (CD40L), LTA (TNFB), VEGFD, NGF, FGF2 (FGFB), IFNA2 (IFNA), IFNB1 (IFNB), IFNG, SERPINE1 (PAI1), RETN, ICAM1, VCAM1, TNFSF10 (TRAIL), and VEGFA (VEGF), among others (Fig. 4A and table S6). The second signature was composed of cytokines that were at relatively high levels in TW preflight, continued to be high inflight, and decreased after return. These cytokines included BDNF, EGF, CXCL5 (ENA78), CXCL1 (GROα), IL2, IL6, LIF, PGDF-BB, TGFA, and TNF (TNFA), with several of them involved in mediating inflammation, cell growth, and cell proliferation, as well as tumor proliferation and vascularization (Fig. 1E and table S6). Of note, IL2 stimulation in CD8 cells activates Hippo signaling (36), and we observed enrichment in this pathway ($q = 0.033$, HGT) when comparing average promoter JSD (a measure of methylation discordance) from TW's preflight with postflight samples in both CD4 and CD8 cells (table S4). The third signature of inflammation was seen immediately after landing (R +0 and R+4), with up to eightfold changes for CCL2 (MCP-1), C-reactive protein (CRP), and IL1RN (IL1RA; fig. S8, A to C; ANOVA, $q < 0.001$; table S8). Notably, CCL2 levels

were increased at R+0, whereas CRP levels rose at R+0 and continued to rise at R+4 days. IL1RA levels only peaked at our R+4 data collection point. All three measures returned to baseline levels by the R+36 collection. During both inflight and postflight periods in TW, we detected increased levels of lysophospholipids containing proinflammatory omega-6 20:4 fatty acid (arachidonic acid) (37), together with a decrease in lysophospholipids containing anti-inflammatory omega-3 20:5 fatty acid (eicosapentaenoic acid) (38), suggestive of an increased inflammatory status (Fig. 4B and table S3).

Finally, we performed a vaccination response experiment to compare the effect of an influenza immunization in the spaceflight environment with that on Earth on the T cell receptor (TCR) repertoires in both subjects with the 2015–2016 trivalent unadjuvanted flu vaccination. Samples were obtained from TW and HR before and ~10 days after a trivalent flu immunization at three time points over the duration of the study. TW was sampled both on Earth (years 1 and 3) and on the ISS (year 2). For samples collected on Earth, repertoires for CD4 and CD8 T cells were separated, whereas frozen PBMCs from the ISS were expected to be a mixture of CD4 and CD8 repertoires. Vaccination-responsive clones were identified by matching complementarity-determining regions (CDR3s) pre- and postvaccination for each subject and cell type, with z scores as measures of change in a one-tailed approach. There were no significant differences (FDR > 0.05) in the percentage of unique CD4 or CD8 T cell receptor sequences (vaccination-responsive clones) that were noted as recruited by vaccination at 6 months inflight from the total PBMC fraction when compared with preflight and postflight responses in TW (Fig. 4C and fig. S9).

Taxonomic and functional microbial shifts during spaceflight

Changes over time in the gastrointestinal (GI) microbiota were examined with shotgun metagenome sequencing of genomic DNA extracted from serial fecal swabs of both subjects over the course of the study (tables S1 and S10). At the taxonomic level of genus, 1364 to 1641 taxa were detected in microbiome samples of both subjects. Although the richness of the fecal microbiome of HR was consistently higher than that of TW ($P < 0.05$, paired Wilcoxon signed-rank test, genus level) for the duration of the study, there were no significant differences between subjects in the Shannon index (SI; an index of diversity) ($P = 0.82$, paired Wilcoxon signed-rank test, genus level). Within TW, there was no decrease in richness or SI in inflight samples relative to preflight and postflight samples [median genera detected 1405.5 versus 1405; median SI ($\log_2$), 2.66 versus 2.42; Fig. 5A].

Fecal microbial communities from both subjects were dominated by bacteria from the phyla Firmicutes and Bacteroidetes, together representing >96% of all annotated sequences recovered. Actinobacterial and Proteobacterial sequences represented 1.97 and 1.27% of annotated sequences, respectively. The ratio of sequences derived from Firmicutes to those derived from Bacteroidetes (F/B ratio) ranged from 0.72 to 5.55. The F/B ratio in TW was higher in inflight samples relative to combined pre- and postflight samples (median F/B ratio 3.21 versus 1.45) but returned to preflight levels postflight (a maximum F/B ratio of 4.60 was observed in TW inflight; Fig. 5A). Yet, all TW F/B ratios were in the range of 0.01 to 5.96 observed in a healthy human cohort (39). Although HR had an increased F/B ratio at the second preflight sampling [ground day (GD)-56; GD-days before TW launch; F/B ratio

of 5.55], this increased ratio was not sustained over time and was low throughout the remainder of the analysis period (range of F/B ratios was 0.72 to 1.76; Fig. 5A). Fecal microbiomes at all sampling time points from both subjects had high relative abundance of bacteria from the genus *Bacteroides* (ranging from 15.4 to 61.0% of reads annotated to the taxonomic level of genus).

When examining diversity among samples (beta diversity), fecal microbial communities of the subjects were significantly different [analysis of similarity (ANOSIM) sample statistic $R = 0.587$, $P = 0.001$] and remained distinct over time (Fig. 5B and fig. S10A). The microbial community structure observed in the four inflight TW samples was significantly different from the pre- and postflight samples combined (ANOSIM, $R = 0.438$, $P = 0.016$; Fig. 5B). No such effect was observed in HR samples (ANOSIM, $R = -0.05$, $P = 0.579$). Similar flight-associated trends were identified in targeted analyses of fungal and viral community structures (fig. S10B) and in analyses of functional gene content across all taxa (Fig. 5C). At the highest resolution of functional gene annotation (SEED function), the subjects had significantly different functional gene content (ANOSIM, $R = 0.456$, $P = 0.003$). For TW, the functional gene content observed in the four inflight samples was significantly different from the preflight and postflight samples (ANOSIM, $R = 0.55$, $P = 0.016$; Fig. 5C). No such change over time was observed for HR (ANOSIM, $R = -0.094$, $P = 0.762$).

To evaluate the extent of microbial community shifts in flight, we identified specific taxonomic groups and gene function features that were significantly altered during the inflight period in both subjects. Specifically, 0.5 to 4.5% of the detected microbial taxa—including 36 species, 13 genera, 8 families, 4 orders, 3 classes, and 3 phyla—were differentially abundant (FDR < 0.05), when inflight samples were compared with the combined pre- and postflight periods (Fig. 5D). However, we found a smaller number of altered microbial groups at each taxonomic level in HR for the same comparison (Fig. 5D). Similar observations were made when analyzing functional gene content. The spaceflight environment significantly (FDR < 0.05, EdgeR) altered the abundance of a moderate fraction (2 to 23%) of gene functional categories at each level in TW inflight compared with the combined preflight and postflight periods. The number of altered gene functional categories was smaller for HR during the inflight-equivalent period (Fig. 5E). Overall, TW's inflight samples had high similarity in taxonomic composition and functional gene content, as assessed with Bray-Curtis similarity (Fig. 5F). The level of similarity within TW's inflight samples was slightly higher than the inflight-equivalent samples from HR for both taxonomic and functional gene annotations ($P = 0.03$ and 0.31, paired Wilcoxon signed-rank test, respectively). Although TW had more similar preflight and postflight microbial communities than HR, these differences were not significant ($P = 0.16$ and 0.13, paired Wilcoxon signed-rank test, for taxonomy and functional gene annotations, respectively; Fig. 5F).

Finally, we examined metabolomic data for corroboration with the microbiome signatures. We observed several small-molecule markers of microbial metabolism in the untargeted LC-MS metabolomics data, including phenyls, secondary bile acid metabolites, and indole containing compounds, some of which are produced solely by microbial metabolism. Some

metabolites, such as 3-indole propionic acid, have anti-inflammatory effects and were observed at lower levels in TW throughout the duration of the study (Fig. 5G and table S3).

Mitochondria-related adaptations during spaceflight

Our integrated analyses identified a number of mitochondria-related changes at the genomic and functional levels related to the 1-year mission. Genic annotation of RNA sequencing (RNA-seq) data (40, 41) revealed higher levels of mtRNA inflight as compared with preflight and postflight (Fig. 6A and fig. S11A). The time spent on the ISS was correlated [coefficient of determination (R^2) = 0.84] with increased mtRNA inflight ($P = 3.6 \times 10^{-6}$, ANOVA). Mitochondrial genome coverage was consistent across all samples (fig. S11B) and validated by qPCR in DNA from blood plasma and qRT-PCR in RNA from PBMCs, supporting this finding further (fig. S11, C to E). We also conducted an extracellular flux assay that monitors real-time changes in the mitochondrial oxygen consumption rate (OCR, a measure of mitochondrial oxidative phosphorylation) by treating muscle cells (L6 cell line) with plasma from the astronauts. The results can be characterized as twofold, whereby the plasma can (i) increase basal respiration (Fig. 6B) and (ii) decrease the spare reserve adenosine triphosphate (ATP) capacity (Fig. 6C). These trends show an increase in ATP-linked respiration, decrease in nonmitochondrial respiration, and no change in maximum respiration (Fig. 6, D and E), which may also reflect the changes in mtRNA levels observed during flight.

Additionally, a significantly increased level of lactic acid ($P = 0.018$; ANOVA) was detected in TW's urine inflight, which returned to baseline postflight. The highest lactic acid levels were observed in TW during the first 15 days and final 14 days of spaceflight (Fig. 6F). GC-MS/MS urine metabolomics data showed an increase in the lactic acid/pyruvic acid ratio (Fig. 6G), indicating a shift from aerobic to anaerobic metabolism. A similar trend in lactic acid levels, as observed in the urine, was also observed in plasma, although only the lactic acid/pyruvic acid ratio was significantly altered in plasma at an FDR of 0.05 (fig. S12, A to C). Lactic acid production promotes higher extracellular acidification rates (42) that, in turn, are associated with increased expression of glycolysis-related genes. We also observed a trend for increased levels of plasma TCA cycle intermediates in the inflight period, such as citric acid and malic acid (FDR < 0.10), compared with preflight and postflight levels (fig. S12, D and E).

Given the previously noted changes in mitochondrial respiration, we examined TW's data for other related signatures. TW exhibited altered gene expression patterns in pathways related to oxygen and reactive species metabolic processes, mitochondrial transport, hypoxia, and apoptotic mitochondrial changes (GSEA, $q < 0.0001$) (table S2). Although differential expression of these genetic pathways is observed in response to hypoxic stimuli in a rodent model (43), the partial pressure of oxygen levels on ISS were near sea-level values (fig. S13).

Cardiovascular changes during spaceflight

Spaceflight-specific changes in cardiovascular structure and function were observed similar to those previously reported (44, 45) in astronauts during long-duration spaceflight,

including a cardiac output increase of 10% (average of spaceflight measurements) (Fig. 7A) and a moderate decrease in systolic and mean arterial pressure (table S7) relative to the upright posture on Earth. Moreover, carotid artery distension developed early in flight during both systole and diastole and persisted throughout the mission (Fig. 7A). Concomitantly, carotid intima-media thickness increased in TW from preflight to inflight and remained thicker 4 days after landing (Fig. 7B). In addition, indices of inflammation, including cytokines [e.g., IL1A, IL1B, IL2, and prostaglandin F2α (PGF2α)] and chemokines, were increased during spaceflight in TW, whereas they remained unchanged in HR across all time points measured (Fig. 7, C and D; fig. S8; and table S6). Biomarkers of oxidative stress were not consistently increased [e.g., oxidized low-density lipoprotein (LDL), myeloperoxidase, and 8-hydroxy-2'-deoxyguanosine (8-OHdG)] in TW during spaceflight (table S8). However, targeted proteomics identified increased levels of two proteins that may be associated with observed changes in vascular wall dimensions. Collagen alpha-1(III) chain (COL3A1) and collagen alpha-1(I) chain (COL1A1) proteins in TW's inflight urine were increased compared with preflight levels, and these values returned to baseline levels postflight (Fig. 7, E and F). We also observed increased COL1A1, from measurements of two separate COL1A1 peptides, by untargeted proteomic analyses (Fig. 7F). This finding is consistent with enrichment of expression levels of genes in the collagen-related pathways [including but not limited to GO term "collagen trimer" and Reactome pathway "collagen formation" in PBMCs (DESeq2, $q < 0.001$)] (table S2). We also observed an increase in the ratio of plasma levels of apoliprotein B (APOB; a major constituent of LDL particles) to apolipoprotein A1 [APOA1; a major constituent of high-density lipoprotein (HDL) particles] during the last 6 months inflight (late inflight; after FD180) in TW, compared with preflight and early inflight (ANOVA, $P = 0.003$, Fig. 7G). These levels decreased postflight and, then, were not significantly different from preflight levels. No significant increase was seen in HR, indicating an association of the APOB/APOA1 ratio with the long duration of the mission.

Body mass, nutrition, and hydration during spaceflight

Baseline and inflight values for HR and TW can be found in table S8. Similar to observations in other astronauts (46), TW lost 7% of his body mass during flight, whereas HR gained ~4% of his body mass over the course of the study (Fig. 8A). TW had decreased urine volume (table S8) and increased urinary aquaporin-2 (AQP2) inflight compared with preflight, which both returned to baseline postflight (Fig. 8B). Serum sodium concentrations (Fig. 8B) and osmolality (Fig. 8C) followed urine AQP2 levels (Fig. 8D) for the duration of the study. TW's energy intake was about 66% of predicted requirements, and beyond the nominal vitamin D supplements provided to all astronauts, he did not report taking vitamin or mineral supplements during the mission. In TW, proteomic analysis revealed a decrease in urine angiotensinogen inflight relative to pre- and postflight that is correlated with the decline of body mass inflight (Fig. 8E).

Bone turnover markers for both breakdown (N-telopeptide; Fig. 8F) and formation (bone-specific alkaline phosphatase; Fig. 8G) increased 50 to 60% in TW during the first 6 months, as previously reported during 4- to 6-month spaceflights (13, 47, 48). However, these markers decreased in the last 6 months of the mission until immediately before landing.

Similar trends were observed for other resorption (e.g., serum CTX-β) and formation markers (e.g., P1NP and osteocalcin; table S8), supporting these data. Bone formation and volume of resistive exercise before the blood draw followed similar trends (Fig. 8H), that is, when exercise volume was lower in the second half of the mission (due to injury), bone formation was correspondingly lower, as expected.

Neuro-ocular changes during spaceflight

Spaceflight resulted in a cephalad fluid shift and ocular changes in TW that were not present in HR. Internal jugular vein cross-sectional area, forehead tissue thickness, cardiac filling, stroke volume, and cardiac output increased, despite an average decrease in mean arterial pressure when compared with values associated with the seated position on Earth (Fig. 9, A and B). Increases in subfoveal choroidal thickness (primary vascular supply of the outer retina) and peripapillary total retinal thickness were observed, indicating retinal edema formation (Fig. 9, C and D). Moreover, although TW exhibited choroidal folds during preflight testing before this mission, the severity of the choroidal folds increased during spaceflight, as quantified by number and depth. These ocular structure parameters were unchanged in HR for the duration of the study, and choroidal folds were not present at the initiation of these data collection sessions (Fig. 9, A to D).

Of relevance to these ocular changes, untargeted proteomics revealed a decrease in urine leucine-rich alpha-2-glycoprotein (LRG1) levels in TW inflight relative to those pre- and postflight (Fig. 9E). LRG1 has been reported to play a role in retinal vascular pathology (49). The predisposition to develop these ocular changes during spaceflight has also been associated with B-vitamin status and the presence of specific single-nucleotide polymorphisms (SNPs) (50). Risk alleles in five SNPs predict incidence of ophthalmic issues (49), and six of the nine risk alleles are present in the twins (50). Furthermore, serum folate, a B vitamin that is often low in astronauts who experienced ophthalmic changes during flight (51), was also low in both TW and HR (Fig. 9F).

Cognitive performance

Continuous high levels of astronaut cognitive performance are critical for mission success. Study subjects performed a computerized cognitive test battery (Cognition) (52) throughout all phases ofthe mission (Fig. 10A). TW'saccuracyand speed scores were measured for the different phases of the mission [preflight, inflight months 1 to 6 (early flight), inflight months 7 to 12 (late flight), and postflight] (Fig. 10B). TW took more risk than HR on the balloon analog risk test (BART) during all phases of the mission, more so inflight compared with preflight and postflight. Compared with HR, TW did not exhibit significant deficits in either speed (−0.7 SD, $P = 0.3518$; Student's t test) or accuracy (−0.2 SD, $P = 0.6678$; Student's t test) across cognitive domains preflight. TW's cognitive speed increased across all cognitive domains early inflight relative to preflight. During the same period, spatial orientation and motor praxis accuracy increased (>1 SD), whereas accuracy of visual object learning and abstract matching decreased (>1 SD) relative to HR. There was no significant decrease in performance from early to late inflight, with the following exceptions: (i) decline (>1 SD) in emotion recognition task (ERT) and digit symbol substitution task (DSST) speed and (ii) decline (>2 SD) in abstract matching (AM) accuracy ($P = 0.0280$; Student's t test;

TW versus HR late flight, Fig. 10C). Performance trends across the study on key accuracy and speed metrics for all 10 tests in the Cognition battery are shown in fig. S14.

Most notably, cognitive speed decreased for all tests except for the DSST, and accuracy decreased for all domains except for spatial orientation postflight. TW's cognitive efficiency (a combination of speed and accuracy across cognitive domains) was similar pre- and inflight relative to HR but was significantly lower postflight ($P = 0.0016$, Student's t test). This postflight decline in cognitive performance persisted up to 6 months postflight in both speed and accuracy domains (Fig. 10C).

Discussion

The NASA Twins Study represents an integrated, multiomics, molecular, physiological, and cognitive portrait of an astronaut and reveals the biomedical responses of a human body during a year-long spaceflight. Our results demonstrate both transient and persistent changes associated with long-duration spaceflight across multiple cell types, tissues, genotypes, and phenotypes. These specific data, as well as the broader biomedical measures and sample collection methods, can now serve as a foundation for scientific and medical assessments of future astronauts, especially for those on prolonged, exploration-class missions.

NASA has announced plans for a Mars mission and a cis-lunar station, which will provide new opportunities for contextualizing human physiological and molecular dynamics during extended spaceflight. Data from this study indicate that at least 10 key physiological processes were influenced by long-duration spaceflight, which serve as targets for development of countermeasure interventions during future exploration-class human space travel. These include (i) body mass and nutrition, (ii) telomere length regulation, (iii) maintenance of genome stability, (iv) vascular health, (v) ocular structural adaptations, (vi) transcriptional and metabolic changes, (vii) epigenetic shifts, (viii) lipid level alterations, (ix) microbiome responses, and(x) cognitive function. These can further be classified as associations that are of potentially (i) low risk, (ii) medium or unknown risk, and (iii) high risk. These risk classifications are made on the basis of the degree of potential functional importance during spaceflight and their persistence for at least 6 months after returning to Earth.

Highly dynamic associations with potentially low risk

Many rapid physiological and molecular changes associated with spaceflight returned to near preflight levels, including average telomere length, body mass, microbiome composition, T cell function, and most cellular and tissue regulation (transcriptional and metabolic). Owing to their pronounced responses during spaceflight, these serve as important potential biomarkers for adaptation of the human body in space but likely represent minimal to low risks for long-duration missions.

Measures of gene function

The majority (91.3%) of the genes that changed expression in CD4, CD8, and LD cells during spaceflight returned to normal ranges within 6 months postflight (Fig. 1B and table S2). In addition, although some epigenetic loci were changed, the genome-wide epigenetic

variance was higher in the ground control than in the flight subject during the 25 months of this study. Furthermore, the observed changes in metabolic levels in plasma returned to baseline postflight. The immune stress indicated by the transcriptional and proteomic data did not seem to impair recruitment of influenza-specific T cells, as evaluated by the response to the midflight vaccination, suggesting that primary immune functions, including chemotaxis, antigen distribution and trafficking, and presentation through the lymphatic system were maintained. Overall, these data show plasticity and resilience for many core genetic, epigenetic, transcriptional, cellular, and biological functions.

Telomere elongation

The spaceflight-specific telomere elongation observed in this study is consistent with similar findings in unrelated astronauts on shorter (~6 month) duration ISS missions, as well as in *Caenorhabditis elegans* flown on the ISS for 11 days (53). Although the underlying mechanisms and potential consequences of such transient telomere elongation are currently unknown, healthy lifestyle factors related to metabolic and nutritional status, physical activity, and weight loss have been associated with longer telomeres (54–60). Consistent with these studies, TW's reduced body mass and increased serum folate levels inflight correlated with telomere lengthening (fig. S15).

Microbiome changes

The GI microbiome can be expected to respond dynamically to changes in diet and other factors, and such variability over time was evident in both subjects. Although each subject maintained individual microbiome characteristics, more changes in microbial community composition and function were found during the flight period in TW than in the equivalent period in HR (Fig. 5). Given the number of significantly changed microbiome features inflight, it is likely that some microbiome changes observed are related to spaceflight. Inflight changes in small-molecule microbiome-derived metabolites (Fig. 5G) also suggest that the microbiome undergoes functional changes in response to spaceflight. Compared with the differences between individuals, the scale of microbiome changes in microbial diversity in TW during flight was relatively small and may be reflective of isolation and dietary change. This is consistent with ground-based studies of volunteers undergoing extended isolation (61, 62). The flight subject showed a significant and spaceflight-specific increase in the F/B ratio; however, this ratio returned to preflight levels within weeks of landing, indicating a rebounding across the microbial ecosystem of the GI tract. Furthermore, the diversity of the microbiome, often considered an indication of microbiome health, was not decreased inflight. The health risks associated with these inflight changes are not known but may be minimal.

Associations with potential mid-level or unknown risk

Several features of long-duration spaceflight represent mid-level or unknown long-term risk, including collagen regulation, intravascular fluid management, and persistent telomere loss and/or critical shortening.

Collagen regulation

To our knowledge, spaceflight-related changes in urinary excretion of COL1A1 and COL3A1 have not previously been observed in astronauts. They are both more than twice the molecular weight of albumin, so whole collagen molecules would filter from blood into the urine poorly (63). They are present in the kidney in relatively low levels. Weightlessness alters loading on cartilage, bone, tendon, skin, vasculature, and the sclera, so these are other potential sources of increased urinary COL1A1 and COL3A1. TW had an increased internal jugular diameter and vascular remodeling of his carotid artery manifested as increased intima-media thickness. COL3A1 is a functionally important component of the vasculature, because defects in the *COL3A1* gene cause blood pooling in the legs and impaired blood pressure responses to standing. Changes in muscle, tendon, bone, and hydrostatic loading during weightlessness provide numerous sites where the body might undergo structural remodeling, leading to increased urinary excretion of COL1A1 and COL3A1.

Intravascular fluid management

Astronauts are at risk for dehydration, which can lead to increased renal stone risk (47). AQP2 controls water transport in the renal collecting duct epithelial cells and is regulated by vasopressin, which is released when the body is dehydrated. A decrease in both food and water intake might be linked to a decreased upper and lower GI motility associated with decreased gravitational force. The return to Earth usually leads to fluid retention and weight gain, and indeed, TW exhibited a modest weight gain in the days after landing. Our study provides evidence that an increase in urinary AQP2 manifests during spaceflight rather than being related to readaptation to the Earth environment and also correlates with serum sodium levels. It is thus likely that increased urine AQP2 was due to high plasma sodium stimulating vasopressin release. AQP2 is regulated by vasopressin, which elicits fluid reabsorption from the urine when activated (64). This renal water reabsorption protein was unable to fully compensate for decreased water intake, leading to an increased plasma sodium concentration and oncotic pressure during flight. TW's increased urine AQP2 may be the result of inflight dehydration or hypernatremia, as indicated by increased plasma sodium levels and measured by osmolality. For future missions, urine AQP2 levels should be monitored in crewmembers to identify who should be considered for potential therapeutic interventions to ameliorate the side effects and physiological complications of dehydration.

During spaceflight, 24-hour urine volumes are generally decreased, secondary to water intake and the low relative humidity onboard the ISS (13). Several of our findings may be associated with the reduced energy intake and weight loss observed in the flight subject, including telomere lengthening (56), decreased angiotensinogen (Fig. 8E), and decreased mitochondrial respiration (Fig. 6). Additionally, DNA methylation was altered inflight at genes enriched in the somatostatin pathway (Fig. 3D). Fasting is known to increase somatostatin transcription (65). Diminished caloric intake decreases many of the hormones related to blood pressure control and metabolism, generally lowering blood pressure and decreasing metabolic rate and muscle growth. TW had increased urine and plasma lactic acid levels inflight and an increased trend for TCA cycle intermediates (malic acid and citric acid), likely due to an intensive exercise regimen (Fig. 6F and fig. S12, D and E).

We also observed changes in urinary excretion of renin-angiotensin pathway proteins. In humans, renin and angiotensin II levels increase with upright posture, and high blood pressure is associated with higher urinary angiotensinogen (66,67). Angiotensin II increases urinary angiotensinogen, probably because it stimulates production of angiotensinogen in the renal tubules. Astronauts are not “upright” in space, and an astronaut’s blood pressure is lower in space (44). Indeed, we observed decreased angiotensinogen (fig. S5A) and lower blood pressure in TW inflight (table S7). The observed reduction in renin receptor protein in the urine during flight is likely due to a similar pathway that lowers angiotensinogen inflight.

Persistent telomere loss and/or critical shortening

The rapid (<48 hours) shortening of TW’s telomeres upon return to Earth coincided with the extreme stresses associated with landing and a heightened inflammatory response, a well-established contributor to telomere shortening (68). The transient nature of spaceflight-induced telomere elongation was also apparent in TW’s postflight telomere length distributions, which rapidly shifted back toward baseline upon return. However, there were substantial decreases in the number of telomeres detected, suggesting persistent telomere loss and/or increased numbers of critically short telomeres. Consistent with these observations, ISS astronauts in general tend to have significantly shorter telomeres alter flight than before. The potential importance of such shifts in telomere length (elongation and accelerated shortening or loss) is underscored by accumulating evidence that supports telomere length not only as a robust biomarker of aging but also as a determinant of age-related diseases, such as cardiovascular disease and cancer (69). Because such metrics can inform overall health, monitoring telomere length dynamics represents an important element of evaluating health and potential long-term risk for future astronauts.

Associations with potentially high risk

Returning to Earth is an especially stressful event that represents one of the greatest physiological challenges of spaceflight. In the immediate postlanding period, manifestations of this include exaggerated or impaired cardiovascular, musculoskeletal, and stress and inflammatory responses (6, 11, 13, 70). Furthermore, there are concerns related to both the recovery period and to the long-term consequences of spaceflight with regard to cardiovascular, ocular, and cognitive systems, including the molecular features of astronauts’ cells.

Spaceflight-associated neuro-ocular syndrome

As of May 2017, about 40% of astronauts have experienced one or more of the following ocular issues: optic disc edema, hyperopic shifts, globe flattening, cotton-wool spots, or choroidal folds (16). Multiple hypotheses have been proposed to explain the development of these symptoms, collectively referred to by NASA as SANS (16), including the spaceflight-induced cephalad fluid shift and associated adaptations. Distension of and increased pressure in the internal jugular vein were observed inflight in TW, at levels similar to those while supine on Earth. The result of this vascular engorgement may contribute to congestion of the vasculature supplying the retina, as suggested by the thickening of subfoveal choroid (14). Importantly, given that normal gravity and hydrostatic pressure gradients are not present

onboard the ISS, there is no relief from the headward fluid shift as would be expected on Earth during normal postural changes. Indeed, clinical reports of optic disc edema from fundoscopy were confirmed by our optical coherence tomography measures of increased total peripapillary retinal thickness. Combined with worsening of choroidal folds from pre- to inflight, TW demonstrated symptoms that are consistent with SANS. Although some ocular changes recover in the postflight recovery period, such as choroidal congestion and retinal nerve fiber layer thickening, some ocular findings, including choroidal folds, may persist from a previous long-duration spaceflight mission (16) and worsen in a subsequent mission (71), as was observed in TW. By contrast, HR did not develop similar ocular findings across the measurements obtained during this study, despite participating in four previous short-duration space shuttle missions. Thus, any changes that HR might have experienced previously either did not manifest, despite HR expressing the same risk alleles as his twin brother, or had resolved since his last mission. These observations support the "multiple hit" hypothesis (72) that genetics presents a predisposing factor that manifests pathologically only when present in combination with one or more other physiological, biochemical, and/or environmental factors, including duration of continuous exposure (e.g., longer than a 2-week space shuttle flight).

Vascular physiology

The cephalad fluid shift that occurs when astronauts enter the weightless environment is hypothesized to be the initiating event associated with cardiovascular adaptations to spaceflight. Secondary to the loss of hydrostatic gradients due to weightlessness, about 2 liters of fluid move from the lower to the upper body (3, 7). Although some variability between crewmembers exists, this headward fluid shift is described as the appearance of a "puffy face" and "bird legs" in many crewmembers. Despite a relative decrease in plasma and blood volume (4, 5) and a reduction in blood pressure (44), stroke volume and cardiac output increase, and arteries and veins in the upper body are distended (73). Results from astronauts participating in 4- to 6-month missions reveal increased carotid intima-media thickness (45)and vascular stiffness (74)that are suggested to be related to increased oxidative stress, inflammation, and insulin resistance. Similar trends were observed in 10 astronauts completing 4- to 6-month missions, with carotid intima-media thickening observed early inflight that did not appear to increase further near the end of the mission (45). Consistent with these findings, similar adaptations developed in TW, as there was a rapid increase in carotid intima-media thickness after launch. However, the carotid intima-media layer did not continue to thicken during the latter half of the mission (from 6 to 12 months inflight). Whether the intima-media thickening is irreversible and represents an increased cardiovascular and cerebrovascular disease risk (75) across the lifetime of an astronaut is not yet known, especially because prediction of clinical events among otherwise healthy individuals is difficult. Similarly, we observed a pre- to inflight increase in the APOB/APOA1 ratio, specifically in the latter half of the mission, that might be suggestive of an increased cardiovascular disease risk in TW (76–78), but the long-term health consequences are as yet unknown. Measurements obtained during recovery from spaceflight in this subject, together with measurements taken from other astronauts in a companion study, will provide important information about the course of cardiovascular disease risk factors. Recent epidemiological studies suggest that astronauts do not have an increased

cardiovascular morbidity (79) or mortality risk (80), but there is insufficient data to draw conclusions regarding astronauts who participate in long-duration missions; the vast majority of subjects in these investigations participated in short-duration missions.

Postflight stress and inflammatory response

The molecular features assessed in TW were consistent with a stress and inflammatory response in the days after landing. In particular, TW exhibited an increase in CRP from 1 to 19 mg/dl and increased levels of IL1RA (fig. S8, B and C, and table S8). TW's cytokine signature was also consistent with an inflammatory response upon return to Earth (Fig. 4A and fig. S8D). The stress and inflammatory response may have preceded the return phase of the mission as the increase in lysophospholipids containing proinflammatory fatty acids suggested a heightened inflammatory state during flight as well (Fig. 4B). Furthermore, TW's average urine sodium excretion from FD300 through FD334 was 147 mmol/day (table S8). On R+0, sodium excretion decreased to 47 mmol/day despite being given intravenous saline, as is routine protocol at landing (81), as well as access to enough fluid intake to increase his urine volume from 1313 to 2999 ml. TW did not have blood volume measures until R+12; however, on the basis of previous data on crewmembers on long-duration spaceflight (5), TW's blood volume at R+0 was likely low. His plasma sodium concentration decreased from 146 to 138 mmol/liter on R+0 (table S8), consistent with urine sodium output not being decreased, likely owing to low plasma sodium. The observed two-thirds decrease in urine sodium excretion on landing, despite being provided intravenous saline, is a common response to volume depletion.

Genomic instability

Multiple lines of evidence revealed ongoing genome instability and rearrangement, potentially indicative of long-term molecular and/or adverse health effects of long-duration spaceflight. Notably, and consistent with reported space radiation exposure and inflight DNA damage responses, TW's chromosomal translocation and inversion frequencies were increased during flight and remained increased postflight. These findings are in agreement with reports of chromosomal translocations in individual astronauts (32), as well as with the proposal that inversions, together with their reciprocal counterpart small interstitial deletions, represent mutational signatures of radiation exposure (82). Furthermore, in vitro experiments have demonstrated that exposures to high-LET protons can evoke telomere lengthening (83), that low-LET gamma-ray exposures induce telomerase-dependent enrichment of putative stem and progenitor cell populations, and that low-dose rate irradiation of PBMCs shifts telomere length distributions toward cell populations with longer telomeres (24). Therefore, radiation- and DDR-induced changes in cell population dynamics, rather than telomere lengthening per se, may at least partially contribute to the telomere elongation observed during flight.

Dysregulated gene expression

Interestingly, the number of DEGs (table S2) in the 6- to 12-month inflight period was almost sixfold higher than in the 0- to 6-month inflight period in unsorted PBMCs (DEGs $q < 0.01$, DESeq2), indicating that the latter half of a year-long mission induces a far greater number of transcriptional changes. Furthermore, a distinct subset of genes did not return to

preflight levels within 6 months of return to Earth (811 genes across different cell types), including genes related to immune function and DNA repair, representing candidate genes that may be altered for an extended period of time as a result of long-term spaceflight exposure.

Cognitive decline

Finally, our findings suggest that the cognitive performance effects of prolonging mission duration from 6 to 12 months may be limited to a few domains. However, this extended mission duration may negatively affect cognitive performance postflight, which could have implications for safe mission operations (e.g., after a landing on Mars). Automation of postflight operational procedures on future missions could help mitigate such risks. In addition to reexposure to Earth'sgravity, the postflight period can be demanding for astronauts owing to participation in research studies and media events. It is unclear how strongly each of the above factors contributed to the observed decline in the flight subject's cognitive performance postflight.

Future missions and conclusions

This study has generated a unique, diverse biomedical dataset, despite the fact that studying the effects of space travel on the human body is challenging. Samples collected on the ISS were either frozen at −80°C and kept as such for the duration of the mission or returned under ambient conditions to Earth. Sample return from the ISS involved unavoidable transit times (~45 hours) through Earth's atmosphere and intercontinental travel, sometimes with unknown transit conditions (e.g., temperature and vibration). This resulted in significant changes, such as loss of telomerase activity. However, DNA integrity was intact and telomere length was unaffected (fig. S6, F to H).

Given our results, it is expected that astronauts conducting exploration-class missions could experience risks from mitochondrial dysfunction, immunological stress, vascular changes and fluid shifts, and cognitive performance decline, as well as alterations in telomere length, gene regulation, and genome integrity. Given the limitations in analyzing a single spaceflight subject, studies of additional astronauts on long-duration (≥12 month) missions are needed to confirm these findings and resolve outstanding questions. If confirmed, any biological, biophysical, or pharmacological countermeasures that reduce these risks should be considered for development and implementation. There is even less data, or no data, on astronauts who might be at increased risk owing to space radiation exposure associated with exploration missions beyond the protection afforded by Earth's magnetic field (84), including differences between a 1-year spaceflight in low Earth orbit and a 3-year Mars mission. Therefore, future studies with varying durations and longer periods of exposure (>1 year) will be required to determine the manner by which those risks will change (e.g., linear or exponential) and to establish appropriate safety thresholds.

These results represent an integrated portrait of molecular, physiological, and behavioral adaptations and challenges for the human body during extended spaceflight and are important to individual astronauts and to many groups at NASA (e.g., ISS Program, Space Medicine, and the Human Research Program) for planning other ISS missions. These data

can be of immediate use by investigators and groups around the world planning future human spaceflight missions. Moreover, future year-long ISS missions would provide additional subjects and materials for subsequent studies and interpretation in support of future Mars missions. However, the opportunity to have an identical twin as a control for a spaceflight study is not currently planned nor expected. Thus, this study and its methodologies represent a uniquely controlled and integrated framework for comprehensively quantifying astronaut biology in space.

Materials and methods summary

The materials and methods are briefly summarized here; expanded materials and methods are included in the supplementary materials. Data were generated across human and microbial cells, including isolations of stool, saliva, skin, urine, blood, plasma, PBMCs, and immune cells that are CD4+, CD8+, and CD19+ enriched and lymphocyte-depleted (LD), from AutoMACS magnetic bead separation and validated by FACS (fig. S1). Molecular techniques included assessments of telomere length, telomerase activity, and chromosome aberration frequencies (qRT-PCR T:A, qRT-PCR TRAP, Telo-FISH, and dGH), WGBS, RNA-seq (polyA, riboRNA, and miRNA), mitochondrial quantification (qPCR and qRT-PCR), shotgun metagenome sequencing of fecal microbiome, targeted proteomics (LC-MS), untargeted proteomics (PECAN, MaxQuant for urine and SWATH-MS for plasma), targeted metabolomics (GC-MS), untargeted metabolomics (LC-MS), mitochondrial respiration (Seahorse XF), oxidative state measures (EPR), TCR and BCR (T cell and B cell receptor repertoire) profiling, 10 cognitive tests (motor praxis, visual object learning, fractal 2-back, abstract matching, line orientation, emotion recognition, matrix reasoning, digit symbol substitution, balloon analog risk, and psychomotor vigilance), vascular and ocular measures by ultrasound and optical coherence tomography, respectively, and a wide range of other biometrics (e.g., nutrition, height, and weight). Finally, a large set of biochemical profiles were measured pre-, in-, and postflight for both subjects: body mass, height, energy intake, vitamin levels (A, B6, B12, C, D, and E and 1-carbon metabolites), minerals (copper, ceruloplasmin, selenium, zinc, calcium, phosphorus, magnesium, and iodine), iron levels (ferritin, transferrin, transferrin receptors, Hgb, Hct, MCV, TIBC, and hepcidin), urine proteins (total, albumin, TTR, RBP, creatinine, metallothionein, 3-MH, nitrogen, and fibrinogen), bone markers (BSAP, PTH, OPG, RANKL, P1NP, sclerostin, and osteocalcin), collagen crosslinks (NTX, CTX, and DPD), oxidative stress and antioxidant capacity (8-OHdG, PGF2α, GPX, SOD, TAC, oxLDL, total lipid peroxides, heme, and glutathione), protein carbonyls (myeloperoxidase, lp-PLA2, neopterin, and beta-2 microglobulin), hormones and immune system markers (cytokines, testosterone, estradiol, DHEA/S, cortisol, IGF1, leptin, thyroid hormones, angiotensin, aldosterone, ANP, PRA, and insulin), and general urine chemistry (Na, K, and Cl ions; uric acid; cholesterol; triglyceride; HDL; LDL; phospholipids; renal stone risk; liver enzymes; hsCRP; NAD/P; and pH). Together, these data span 25 months for the flight subject twin (TW), who was compared with himself, either preflight, inflight, or postflight, and also with his twin control (HR) on Earth using generalized linear models (GLM), DESeq2, and fuzzy *c*-means clustering for longitudinal trends. All *P* values were corrected for multiple testing using a FDR of 0.05 or 0.01, and *q* values are reported in all tables.

Supplementary Material

Refer to Web version on PubMed Central for supplementary material.

Authors

Francine E. Garrett-Bakelman[1,2,*], Manjula Darshi[3,*], Stefan J. Green[4,*], Ruben C. Gur[5,*], Ling Lin[6,*], Brandon R. Macias[7,*], Miles J. McKenna[8,*], Cem Meydan[1,9,*], Tejaswini Mishra[6,*], Jad Nasrini[5,*], Brian D. Piening[6,*,†], Lindsay F. Rizzardi[10,*,‡], Kumar Sharma[3,*], Jamila H. Siamwala[11,*,§], Lynn Taylor[8,*], Martha Hotz Vitaterna[12,*], Maryam Afkarian[13], Ebrahim Afshinnekoo[1,9], Sara Ahadi[6], Aditya Ambati[6], Maneesh Arya[7], Daniela Bezdan[1,9], Colin M. Callahan[10], Songjie Chen[6], Augustine M. K. Choi[1], George E. Chlipala[4], Kévin Contrepois[6], Marisa Covington[14], Brian E. Crucian[14], Immaculata De Vivo[15], David F. Dinges[5], Douglas J. Ebert[7], Jason I. Feinberg[10], Jorge A. Gandara[1], Kerry A. George[7], John Goutsias[10], George S. Grills[1,¶], Alan R. Hargens[11], Martina Heer[16,#], Ryan P. Hillary[6], Andrew N. Hoofnagle[17], Vivian Y. H. Hook[11], Garrett Jenkinson[10,**], Peng Jiang[12], Ali Keshavarzian[18], Steven S. Laurie[7], Brittany Lee-McMullen[6], Sarah B. Lumpkins[19], Matthew MacKay[1], Mark G. Maienschein-Cline[4], Ari M. Melnick[1], Tyler M. Moore[5], Kiichi Nakahira[1,††], Hemal H. Patel[11], Robert Pietrzyk[7], Varsha Rao[6], Rintaro Saito[11,‡‡], Denis N. Salins[6], Jan M. Schilling[11], Dorothy D. Sears[11], Caroline K. Sheridan[1], Michael B. Stenger[14], Rakel Tryggvadottir[10], Alexander E. Urban[6], Tomas Vaisar[17], Benjamin Van Espen[11], Jing Zhang[6], Michael G. Ziegler[11], Sara R. Zwart[20], John B. Charles[14,§§], Craig E. Kundrot[21,§§], Graham B. I. Scott[22,§§], Susan M. Bailey[8,§§], Mathias Basner[5,§§], Andrew P. Feinberg[10,§§], Stuart M. C. Lee[7,§§], Christopher E. Mason[1,9,23,24,§§], Emmanuel Mignot[6,§§], Brinda K. Rana[11,§§], Scott M. Smith[14,§§], Michael P. Snyder[6,§§], Fred W. Turek[12,§§]

Affiliations

[1]Weill Cornell Medicine, New York, NY, USA

[2]University of Virginia School of Medicine, Charlottesville, VA, USA

[3]Center for Renal Precision Medicine, University of Texas Health, San Antonio, TX, USA

[4]University of Illinois at Chicago, Chicago, IL, USA

[5]University of Pennsylvania Perelman School of Medicine, Philadelphia, PA, USA

[6]Stanford University School of Medicine, Palo Alto, CA, USA

[7]KBRwyle, Houston, TX, USA

[8]Colorado State University, Fort Collins, CO, USA

[9]The Bin Talal Bin Abdulaziz Alsaud Institute for Computational Biomedicine, New York, NY, USA

[10]Johns Hopkins University, Baltimore, MD, USA

[11]University of California, San Diego, La Jolla, CA, USA

[12]Northwestern University, Evanston, IL, USA

[13]University of California, Davis, Davis, CA, USA

[14]National Aeronautics and Space Administration (NASA), Houston, TX, USA

[15]Harvard T.H. Chan School of Public Health, Boston, MA, USA

[16]University of Bonn, Bonn, Germany

[17]University of Washington, Seattle, WA, USA

[18]Rush University Medical Center, Chicago, IL, USA

[19]MEI Technologies, Houston, TX, USA

[20]University of Texas Medical Branch, Galveston, TX, USA

[21]Space Life and Physical Sciences Division, NASA Headquarters, Washington, DC, USA

[22]National Space Biomedical Research Institute, Baylor College of Medicine, Houston, TX, USA

[23]The Feil Family Brain and Mind Research Institute, New York, NY, USA

[24]The WorldQuant Initiative for Quantitative Prediction, New York, NY, USA

ACKNOWLEDGMENTS

The National Space Biomedical Research Institute partnered with NASA to support this study during the solicitation, design, implementation, and analysis phases via the provision of scientific expertise. We thank S. Horner and N. Gokhale from Duke University Medical Center (Durham, NC, USA) for mtRNA validation assistance, I. Tulchinsky, and the Genomics, Epigenomics, and Applied Bioinformatics Core Facilities at Weill Cornell Medicine for sequencing and data services. We thank the NASA JSC Nutritional Biochemistry Lab personnel, especially Y. Bourbeau, who led efforts on this project for project coordination, sample collection, processing, and analysis; the Cardiovascular and Vision Laboratory personnel for the collection and analysis of vascular, ocular, and fluid shifts data; the NASA Human Research Program's International Space Station Medical Project Team for their invaluable work to coordinate all of sample and data collection scheduling activities on the ground and during flight; D. Mollicone and C. Mott from Pulsar Informatics Inc., E. Hermosillo, and S. McGuire for support of the Cognition measures; Y.-R. Hasson from the Stanford Human Immune Monitoring Center for advice and support on cytokine profiling data; K. Bettinger from Stanford University for support with the Stanford Twins data repository; P. R. Kiela, D. Laubitz (University of Arizona), and E. Song (Northwestern University) for support of the Microbiome project sample collection; K. Kunstman (University of Illinois at Chicago) for shotgun metagenome library preparation and sequencing; S. Mehta (University of Illinois at Chicago) for help in statistical analysis; and J. Kim for laboratory support in targeted metabolomics. We thank the DRC Quantitative and Functional Proteomics Core and the UW Nutrition and Obesity Research Center for performing proteomics assays and New England Biolabs (NEB) for support. We thank J. X.-J. Yuan at the University of Arizona, Tuscon, for providing his support and laboratory for the Tucson sample collections. We thank J. Krauhs for her editorial assistance with the one-page summary. K.S. is also affiliated with the South Texas U.S. Department of Veterans Affairs as a staff physician.

Funding: The study was supported by NASA: NNX14AH51G [all Twins Study principal investigators (PIs)]; NNX14AB02G (S.M.B.); NNX14AH27G/NCC 9-58 (M.B.); NN13AJ12G (A.R.H.); NNX14AN75G (S.M.C.L.); NNX17AB26G, NNX17AB26G, and TRISH: NNX16AO69A:0107 and NNX16AO69A:0061 (C.E.M.); NNX14AH52G (M.P.S.); and NNX14AH26G (F.W.T.). Additional support was provided by NIH grants AG035031, NIH/NIDDK P30 DK017047, and P30 DK035816 (K.S.); NSF grant CCF-1656201 (J.G.); and DLR space program grant 50WB1535 (M.H.), as well as the Bert L. and N. Kuggie Vallee Foundation, the WorldQuant Foundation, The Pershing Square Sohn Cancer Research Alliance, and the Bill and Melinda Gates Foundation (OPP1151054) for funding (C.E.M.).

Appendix

Author contributions: F.E.G.-B., M.D., S.J.G., R. C.G., L.L., B.R.M., M.J.M., C.M., T.M., J.N., B.D.P., L.F.R., K.S., J.H.S., L.T., and M.H.V. led the investigator teams across the study. *Conceptualization:* G.B.I.S., C.E.K., and J.B.C.; S.M.B. (Twins Study PI; Telomeres, Telomerase, DNA damage/cytogenetics); M.B. (Twins Study PI; Cognition); S.M.C.L. [Twins Study PI, Cardiovascular and Oxidative Stress (Cardio Ox); Twins Study co-investigator (Co-I), Fluid Shifts and Ocular]; S.M.S. and S.R.Z. (Biochem Profile); M.H. (Biochem Profile); A.P.F. (Twins Study PI; Epigenetics); M.B.S. (Fluid Shifts NASA site PI and Cardio Ox Co-I); B.R.M. (Fluids Shifts, Co-I); D.J.E. (Fluid Shifts, Co-I); B.K.R. (PI, Fluids Shifts and Co-I, Cardio Ox); I.D.V. (Co-I, Cardio Ox); D.D.S. (Co-I, Cardio Ox); K.S. (Co-I, Targeted Metabolomics, Cardio Ox); A.R.H. (Co-I, Fluid Shifts and Cardio Ox); V.Y.H.H. (Co-I, Fluid Shifts Proteomics); H.H.P., J.H.S., and J.M.S. (Fluid Shifts; Mitochondrial Function); T.V., A.N.H., and M.Af. (Targeted Urine Proteomics); M.P.S. (Twins Study PI; Untargeted Plasma Metabolomics and Proteomics, Plasma Cytokine Profiling, Integrative Analysis); T.M. (Untargeted Plasma Metabolomics and Proteomics, Plasma Cytokine Profiling, Integrative Analysis); B.D.P. (Integrative Analysis); S.J.G., A.K., F.W.T., and M.H.V. (Microbiome); C.E.M. (Twins study PI; Transcriptome, and Integration); and D.D.S. (Co-I, Cardio Ox). *Data Curation:* S.M.B. (Twins Study PI; Telomeres, Telomerase, DNA damage/cytogenetics); M.B. (Twins Study PI; Cognition); J.I.F. and L.F.R. (Epigenetics); S. R.Z. (Biochem Profile); R.P.H. (Immune Response); S.M.C.L. (Twins Study PI, Cardiovascular; Twins Study Co-I, Fluid Shifts and Ocular); S.S.L. (Fluids Shifts and Ocular, Co-I); B.R.M. (Fluids Shifts and Ocular, Co-I); D.J.E. (Fluid Shifts and Ocular, Co-I); B.K.R. (PI, Fluids Shifts and Ocular; Co-I, Cardio Ox); I.D.V. (Co-I, Cardio Ox); K. S. (Co-I, Cardio Ox); M.D. and R.S. (Targeted Metabolomics); J.H.S. and J.M.S. (Mitochondrial Function); D.N.S. (Integrative Analysis); G.E.C., S.J.G., P.J., M.G.M.-C., and M.H.V. (Microbiome); A.N.H. and T.V. (Urine Proteomics); T.M. (Untargeted Plasma Metabolomics and Proteomics, Plasma Cytokine Profiling, Integrative Analysis); S.A. (Untargeted Plasma Proteomics); K.C. (Untargeted Plasma Metabolomics); C.M. and C.E.M. (Twins study PI); E.A., D.B., F.E.G.-B., and M.M. (Transcriptome); B.D.P. (Integrative Analysis); and D.N.S. (Integrative Analysis). *Formal Analysis:* S.M.B. (Twins Study PI; Telomeres, Telomerase, DNA damage/cytogenetics), M.J.M. (Telomeres and Cytogenetics; FISH), L.T. (Telomeres and Telomerase; qRT-PCR); M.B. (Twins Study PI; Cognition); J.N. (Cognition); A.P.F., F.R., G.J., and J.G. (Epigenetics); R.P.H. (Immune Response); S.M.C.L. (Twins Study PI, Cardio Ox; Twins Study Co-I, Fluid Shifts and Ocular); S.M.S. and S.R.Z. (Biochem Profile); S.S.L. (Fluids Shifts and Ocular, Co-I); B.R.M. (Fluids Shifts and Ocular, Co-I); B.K.R. (PI, Fluids Shifts and Ocular; Co-I, Cardio Ox); M.G.Z. (Cardio Ox); I. D.V. (Co-I, Cardio Ox); D.D.S. (Co-I, Cardio Ox); K.S., M.D., and R.S. (Targeted Metabolomics); H.H.P., J.H.S., and J.M.S. (Mitochondrial Functional Assays); T.V. and A.N.H. (Urine Proteomics); T.M. (Untargeted Plasma Metabolomics and Proteomics, Plasma Cytokine Profiling, Integrative Analysis); S.A. (Untargeted Plasma Proteomics); K.C. (Untargeted Plasma Metabolomics); B.D.P. (Integrative Analysis); R.S. and M.D. (Metabolomics); P.J. (Microbiome); E.M., L.L., and A.A. (Vaccination study); and C.M., C.E.M., and A.M. (Transcriptome, Integrative Analysis). *Funding and Acquisition:* S.M.B. (Twins Study PI; Telomeres, Telomerase, DNA damage/cytogenetics); M.B. (Twins

Study PI; Cognition); D.F.D. (Cognition); R.C.G. (Cognition); S.M.S. and S.R.Z. (Biochem Profile); M. H. (Biochem Profile); A.P.F. (Twins Study PI, Epigenetics); J.G. (Epigenetics); S.M.C.L. (Twins Study PI, Cardio Ox; Twins Study Co-I, Fluid Shifts and Ocular); M.B.S. (Fluid Shifts and Ocular NASA Site PI; Cardio Ox Co-I); B.R.M. (Fluids Shifts and Ocular; CardioOX, Co-I); D. J.E. (Fluid Shifts and Ocular, Co-I); B.K.R. (PI, Fluids Shifts and Ocular; UCSD Site PI, Cardio Ox); I.D.V. (Co-I, Cardio Ox); A.R.H. (Co-I, Fluid Shifts and Ocular; Cardio Ox); M.P.S. (Twins Study PI, Untargeted Plasma Metabolomics and Proteomics, Plasma Cytokine Profiling, Integrative Analysis); V.Y.H.H. (Co-I, Fluid Shifts); F.W.T. (PI), M.H.V. (Co-I) (Microbiome), C.E.M. (PI, Transcriptome), C.M., F.E.G.-B., and A. M.M. (Co-I, Transcriptome), G.S.G. (Co-I, Transcriptome); D.D.S. (Co-I, Cardio Ox); and B.R.M. (Co-I, Fluid Shifts and Ocular; Cardio Ox). *Investigation:* M.J.M. (Telomeres and Cytogenetics; FISH), L. T. (Telomeres and Telomerase; qRT-PCR); M.B. (Twins Study PI; Cognition); J.N. (Cognition); R.C.G. (Cognition); S.M.S. and S.R.Z. (Biochem Profile); L.F.R., R.T., C.M.C., and J.I.F. (Epigenetics); S.M.C.L. (Twins Study PI, Cardio Ox; Twins Study Co-I, Fluid Shifts and Ocular); M. B.S. (Fluid Shifts and Ocular; Cardio Ox, Co-I); S.S.L. (Fluids Shifts and Ocular, Co-I); B.R.M. (Fluids Shifts and Ocular, Co-I); D.J.E. (Fluid Shifts and Ocular, Co-I); B.K.R. (PI, Fluids Shifts and Ocular; Co-I, Cardio Ox); M.G.Z. (Cardio Ox); I.D.V. (Co-I, Cardio Ox); K.S., M.D., B. V.E. (Targeted Metabolomics); M.D. (Cardio Ox); B.V.E. (Cardio Ox); A. R.H. (Co-I, Fluid Shifts and Ocular; Cardio Ox); H.H.P., J.H.S., and J. M.S. (Mitochondrial Function Assays); Fluid Shifts); T.V. and A.N.H. (Urine Proteomics); T.M. (Untargeted Plasma Metabolomics and Proteomics, Plasma Cytokine Profiling, Integrative Analysis); B.D.P. (Integrative Analysis); S.A. (Untargeted Plasma Proteomics); V.R. (Plasma Cytokine Profiling); S.J.G. and P.J. (Microbiome); K.C., B.L.M., and S.C. (Untargeted Plasma Metabolomics); E.M., L.L., and A.A. (Vaccination study); and C.E.M., G.S.G., D.B., F.E.G.-B., and A.M.M. (Transcriptome, Integrative Analysis). *Methodology:* M.J.M. (Telomeres and Cytogenetics; FISH), L.T. (Telomeres and Telomerase; qRT-PCR); M.B. (Twins Study PI; Cognition); J.N. (Cognition); R.C.G.(Cognition); T. M.M. (Cognition); G.J., J.G., and J.I.F. (Epigenetics); S.M.C.L. (Twins Study PI, Cardio Ox; Twins Study Co-I, Fluid Shifts and Ocular); M.B.S. (NASA Site PI, Fluid Shifts and Ocular; Cardio Ox, Co-I); S.S.L. (Fluids Shifts and Ocular, Co-I); B.R.M. (Fluids Shifts and Ocular; Cardio Ox, Co-I); D.J.E. (Fluid Shifts and Ocular, Co-I); B. K.R. (PI, Fluids Shifts and Ocular; Co-I, Cardio Ox); M.G.Z. (Cardio Ox); I. D.V. and D.D.S. (Co-I, Cardio Ox); A.R.H. (Co-I, Fluid Shifts and Ocular; Cardio Ox, Co-I); H.H.P., J.H.S., and J.S. (Mitochondrial Function Assays); T.V., A.N.H., and M.Af. (Urine Proteomics); V.Y.H.H. (Proteomics); S.J.G., A.K., F.W.T., and M.H.V. (Microbiome); T.M. (Untargeted Plasma Metabolomics and Proteomics, Plasma Cytokine Profiling, Integrative Analysis); S.A. (Untargeted Plasma Proteomics); V.R. (Plasma Cytokine Profiling); K.C. (Untargeted Plasma Metabolomics); B.D.P. (Integrative Analysis); E.M., L.L., and A.A. (Vaccination study); C.M. (Transcriptome, Integrative Analysis); K. S. and M.D. (Targeted Metabolomics); S.M.S., S.R.Z., M.H., and B.E.C. (Biochem Profile blood and urine collection, processing, and analysis); S.S., S.Z., K.S., M.D., and D.D.S. (Urine collection and processing); A.M.K.C. and K.N. (Cell-free mtDNA); and L.L., A.F., J. I.F., C.K.S., and F.E.G.-B. (Blood Collection and Processing). *Project administration:* S.M.B. (Twins Study PI; Telomeres, Telomerase, DNA damage/cytogenetics); M.B. (Twins Study PI; Cognition); L.F.R. (Epigenetics); R.P. (subject consent, scheduling, and sample logistics); S.M.C.L.

(Twins Study PI, Cardio Ox; Twins Study Co-I, Fluid Shifts and Ocular); S.M.S. (Twins Study PI, Biochem Profile); M.B.S. (Fluid Shifts and Ocular, Co-I; Cardio Ox, Co-I); S.S.L. (Fluids Shifts and Ocular, Co-I); B.R.M. (Fluids Shifts and Ocular, Co-I); B.K.R. (PI, Fluids Shifts and Ocular; Co-I, Cardio Ox); M.P.S. (Twins study PI; Untargeted Plasma Metabolomics and Proteomics, Plasma Cytokine Profiling, Integrative Analysis); T.M. (Untargeted Plasma Metabolomics and Proteomics, Plasma Cytokine Profiling, Integrative Analysis); B.D.P. (Integrative Analysis); F.W.T. (Microbiome PI); M.H.V. (Microbiome Co-I); C.E.M. and F.E.G.-B. (Blood Collection and Processing and transcriptome studies); K.S. (Targeted Metabolomics); M.Ar.; S.L.; and M.C. *Resources:* S.M.B. (Twins Study PI; Telomeres, Telomerase, DNA damage/cytogenetics), K.G. (Telomeres; sample coordination, NASA IRB); M.B. (Twins Study PI; Cognition); S.M.S. (Biochem Profile); M.H. (Biochem Profile); B.E.C. (Biochem Profile); R.P. (laboratory facilities, materials, and instrumentation); S.M.C.L. (Twins Study PI, Cardio Ox; Twins Study Co-I, Fluid Shifts and Ocular); M.B.S. (Fluid Shifts and Ocular, Co-I; Cardio Ox, Co-I); B.K.R. (PI, Fluids Shifts and Ocular; Co-I, Cardio Ox); I.D.V. (Co-I, Cardio Ox); D.D.S. (Co-I, Cardio Ox); K.S. (Co-I, Cardio Ox); A.R.H. (Co-I, Fluid Shifts and Ocular; Cardio Ox); T.V. (Fluid Shifts and Ocular); A.N.H. (Fluid Shifts and Ocular); G.E.C., S. J.G., P.J., and M.G.M.-C. (Microbiome); M.P.S. (Twins study PI; Untargeted Plasma Metabolomics and Proteomics, Plasma Cytokine Profiling, Integrative Analysis); and D.S. (Data Storage Repository). *Software:* C.E.M. (Transcriptome); D.S. (Data Storage Repository); T. M. (Untargeted Plasma Metabolomics and Proteomics, Plasma Cytokine Profiling, Integrative Analysis); and B.D.P. (Integrative Analysis). *Supervision:* S.M.B. (Twins Study PI; Telomeres, Telomerase, DNA damage/cytogenetics); M.B. (Twins Study PI; Cognition); S.M.S. (Twins Study PI, Biochem Profile); A.P.F. (Twins Study PI); J.G. (Epigenetics); S.M.C.L. (Twins Study PI, Cardio Ox; Twins Study Co-I, Fluid Shifts and Ocular); M.B.S. (Fluid Shifts and Ocular, Co-I; Cardio Ox, Co-I); B.R.M. (Fluids Shifts and Ocular, Co-I); B.K.R. (PI, Fluids Shifts and Ocular; Co-I, Cardio Ox); I.D.V. (Co-I, Cardio Ox); D.D.S. (Co-I, Cardio Ox); K.S. (Co-I, Targeted Metabolomics); H.H.P. (Fluid Shifts and Ocular); J.M.S. (Fluid Shifts and Ocular); M.P.S. (Twins study PI; Untargeted Plasma Metabolomics and Proteomics, Plasma Cytokine Profiling, Integrative Analysis); S.J.G., A.K., F.W.T., and M.H.V. (Microbiome); K.C. (Untargeted Plasma Metabolomics); and C.E.M. and F.E.G.-B. (Blood Collection and Processing and transcriptome studies). *Validation:* M.J.M. (Telomeres and Cytogenetics; FISH), L.T. (Telomeres and Telomerase; qRT-PCR); C.E.M., A.C., K.N., N.S.G., and S.M.H. (mtDNA and mtRNA PCR); M.B. (Twins Study PI; Cognition); J.N. (Cognition); T.M.M. (Cognition); S.M.C.L. (Twins Study PI, Cardio Ox; Co-I, Fluid Shifts and Ocular), S.S.L. (Fluids Shifts and Ocular, Co-I); B.R.M. (Fluids Shifts and Ocular, Co-I); D.J.E. (Fluid Shifts and Ocular, Co-I); B.K.R. (PI, Fluids Shifts and Ocular; Co-I, Cardio Ox); S.M.S. and S.R.Z. (Biochem Profile); I.D.V. (Co-I, Cardio Ox PCR Based Telomere Length); K.S., M.D., and B.V.E. (Targeted Metabolomics); H.H.P. and J.M.S. (Proteomics); and L.L., F.E.G.-B., T.M., and C.M. (Ambient return controls). *Visualization:* S.M.B. (Twins Study PI; Telomeres, Telomerase, DNA damage/cytogenetics); M.J.M. (Telomeres and Cytogenetics; FISH), L.T. (Telomeres and Telomerase; qRT-PCR); M.B. (Twins Study PI; Cognition); J.N. (Cognition); L.F.R. (Epigenetics); S.R.Z. (Biochem Profile); S.M.C.L. (Twins Study PI, Cardio Ox; Twins Study Co-I, Fluid Shifts and Ocular); S.S.L. (Fluids Shifts and Ocular, Co-I); B.R.M. (Fluids Shifts and Ocular, Co-I); B.K.R. (PI, Fluids Shifts

and Ocular; Co-I, Cardio Ox); H.H.P. (Fluid Shifts and Ocular); S.J.G., P.J., and M.G.M.-C. (Microbiome); M.M., C.E.M., and C.M. (Transcriptome, Integrative Analysis); and T.M. (Untargeted Plasma Metabolomics and Proteomics, Plasma Cytokine Profiling, Integrative Analysis). *Writing, original draft:* S.M.B. (Twins Study PI; Telomeres, Telomerase, DNA damage/cytogenetics); K.G. (Telomeres); M.B. (Twins Study PI; Cognition); L.F.R. (Epigenetics); S.M.C.L. (Twins Study PI, Cardiovascular; Twins Study Co-I, Fluid Shifts and Ocular); S.M.S. (Twins Study PI, Biochem Profile); S.R.Z. (Biochem Profile); S.S.L. (Fluids Shifts and Ocular, Co-I); B.R.M. (Fluids Shifts and Ocular, Co-I); D.J.E. (Fluid Shifts, Co-I); B.K.R. (PI, Fluids Shifts and Ocular; Co-I, Cardio Ox); M.G.Z. (Physiology and Proteomics); M.D. (Cardio Ox); T.M. (Untargeted Plasma Metabolomics and Proteomics, Plasma Cytokine Profiling, Integrative Analysis); S.J.G., P.J., A.K., F.W.T., and M.H.V. (Microbiome); H.H.P., J.M.S., and J.H.S. (Mitochondrial Function); C. E.M., C.M., F.E.G.-B., and M.M. (Twins Study PI, Transcriptome, Telomere Validation, Integration); D.D.S., K.S., and M.D. (Metabolomics); and A.H., T.V., and M.Af. (Urine Proteomics). *Editing and manuscript finalization:* F.E.G.-B., L.F.R., T.M., C.M., and C.E.M. *Writing, review and editing:* All authors reviewed and edited the manuscript.

Competing interests: S.M.B. is a cofounder and scientific advisory board member of KromaTiD, Inc. C.E.M. is a cofounder and board member for Biotia, Inc., and Onegevity Health, Inc., as well as an advisor for Abbvie, Inc.; ArcBio; Daiichi Sankyo; DNA Genotek; Karius, Inc.; and Whole Biome, Inc. M.P.S. is a cofounder and scientific advisory board member of Personalis, SensOmics, Qbio, January, and Fitricine, and a scientific advisory board member of Genapsys, Epinomics, Jungla, and Jupyter. A.M.K.C. is a cofounder and stock holder and serves on the Scientific Advisory Board for Proterris, which develops therapeutic uses for carbon monoxide. A.M.K.C. also has a use patent on carbon monoxide. A.M.K.C. served as a consultant for TEVA Pharmaceuticals in July 2018. A.M.M. is a consultant for Janssen.

Data and materials availability: The NASA Life Sciences Data Archive (LSDA) is the repository for all human and animal research data, including that associated with this study. LSDA has a public facing portal where data requests can be initiated (https://lsda.jsc.nasa.gov/Request/dataRequestFAQ). The LSDA team provides the appropriate processes, tools, and secure infrastructure for archival of experimental data and dissemination while complying with applicable rules, regulations, policies, and procedures governing the management and archival of sensitive data and information. The LSDA team enables data and information dissemination to the public or to authorized personnel either by providing public access to information or via an approved request process for information and data from the LSDA in accordance with NASA Human Research Program and JSC Institutional Review Board direction.

REFERENCES AND NOTES

1. Barratt M, Pool SL, Eds., Principles of Clinical Medicine for Space Flight (Springer, 2008).
2. Convertino VA, “Exercise and adaptation to microgravity environments” in Supplement 14: Handbook of Physiology, Environmental Physiology, Comprehensive Physiology (Wiley, 2011), pp. 815–843.

3. Thornton WE, Moore TP, Pool SL, Fluid shifts in weightlessness. Aviat. Space Environ. Med 58, A86–A90 (1987). [PubMed: 3675511]
4. Leach CS et al., Regulation of body fluid compartments during short-term spaceflight. J. Appl. Physiol 81, 105–116 (1996). doi: 10.1152/jappl.1996.81.1.105 [PubMed: 8828652]
5. Meck JV, Reyes CJ, Perez SA, Goldberger AL, Ziegler MG, Marked exacerbation of orthostatic intolerance after long- vs. short-duration spaceflight in veteran astronauts. Psychosom. Med. 63, 865–873 (2001). doi: 10.1097/00006842-200111000-00003 [PubMed: 11719623]
6. Lee SMC, Feiveson AH, Stein S, Stenger MB, Platts SH, Orthostatic intolerance after ISS and Space Shuttle missions. Aerosp. Med. Hum. Perform 86 (suppl. 1), A54–A67 (2015). doi: 10.3357/AMHP.EC08.2015 [PubMed: 26630196]
7. Moore TP, Thornton WE, Space shuttle inflight and postflight fluid shifts measured by leg volume changes. Aviat. Space Environ. Med 58, A91–A96 (1987). [PubMed: 3675513]
8. Perhonen MA et al., Cardiac atrophy after bed rest and spaceflight. J. Appl. Physiol 91, 645–653 (2001). doi: 10.1152/jappl.2001.91.2.645 [PubMed: 11457776]
9. Akima H et al., Effect of short-duration spaceflight on thigh and leg muscle volume. Med. Sci. Sports Exerc 32, 1743–1747 (2000). doi: 10.1097/00005768-200010000-00013 [PubMed: 11039647]
10. Gopalakrishnan R et al., Muscle volume, strength, endurance, and exercise loads during 6-month missions in space. Aviat. Space Environ. Med 81, 91–104 (2010). doi: 10.3357/ASEM.2583.2010 [PubMed: 20131648]
11. Trappe S et al., Exercise in space: Human skeletal muscle after 6 months aboard the International Space Station. J. Appl. Physiol 106, 1159–1168 (2009). doi: 10.1152/japplphysiol.91578.2008 [PubMed: 19150852]
12. Hayes JC, Guilliams ME, Lee SMC, MacNeill KR, Jr ADM, "Exercise: developing countermeasure systems for optimizing astronaut performance in space" in Biomedical Results of the Space Shuttle Program, Risin D, Stepaniak PC, Eds. (NASA/SP-2013-607, NASA, Washington, DC, 2013), pp. 289–314.
13. Smith SM et al., Benefits for bone from resistance exercise and nutrition in long-duration spaceflight: Evidence from biochemistry and densitometry. J. Bone Miner. Res 27, 1896–1906 (2012). doi: 10.1002/jbmr.1647 [PubMed: 22549960]
14. Mader TH et al., Optic disc edema, globe flattening, choroidal folds, and hyperopic shifts observed in astronauts after long-duration space flight. Ophthalmology 118, 2058–2069 (2011). doi: 10.1016/j.ophtha.2011.06.021 [PubMed: 21849212]
15. Zhang LF, Hargens AR, Spaceflight-induced intracranial hypertension and visual impairment: Pathophysiology and countermeasures. Physiol. Rev 98, 59–87 (2018). doi: 10.1152/physrev.00017.2016 [PubMed: 29167331]
16. Stenger MB et al., "Evidence report: Risk of spaceflight associated neuro-ocular syndrome (SANS)" (NASA, Lyndon B. Johnson Space Center, Houston, 2018).
17. Carminati MV, Griffith D, Campbell MR, Sub-orbital commercial human spaceflight and informed consent. Aviat. Space Environ. Med 82, 144–146 (2011). doi: 10.3357/ASEM.2846.2011 [PubMed: 21329032]
18. Contrepois K, Jiang L, Snyder M, Optimized analytical procedures for the untargeted metabolomic profiling of human urine and plasma by combining hydrophilic interaction (HILIC) and reverse-phase liquid chromatography (RPLC)-mass spectrometry. Mol. Cell. Proteomics 14, 1684–1695 (2015). doi: 10.1074/mcp.M114.046508 [PubMed: 25787789]
19. Borresen EC et al., A randomized controlled trial to increase navy bean or rice bran consumption in colorectal cancer survivors. Nutr. Cancer 68, 1269–1280 (2016). doi: 10.1080/01635581.2016.1224370 [PubMed: 27689688]
20. Cawthon RM, Telomere length measurement by a novel monochrome multiplex quantitative PCR method. Nucleic Acids Res. 37, e21 (2009). doi: 10.1093/nar/gkn1027 [PubMed: 19129229]
21. Honig LS et al., Heritability of telomere length in a study of long-lived families. Neurobiol. Aging 36, 2785–2790 (2015). doi: 10.1016/j.neurobiolaging.2015.06.017 [PubMed: 26239175]
22. Lin J et al., Systematic and cell type-specific telomere length changes in subsets of lymphocytes. J. Immunol. Res 2016, 5371050 (2016). doi: 10.1155/2016/5371050 [PubMed: 26977417]

23. Lansdorp PM et al., Heterogeneity in telomere length of human chromosomes. Hum. Mol. Genet 5, 685–691 (1996). doi: 10.1093/hmg/5.5.685 [PubMed: 8733138]
24. Sishc BJ et al., Telomeres and telomerase in the radiation response: Implications for instability, reprograming, and carcinogenesis. Front. Oncol 5, 257 (2015). doi: 10.3389/fonc.2015.00257 [PubMed: 26636039]
25. Greider CW, Blackburn EH, Identification of a specific telomere terminal transferase activity in Tetrahymena extracts. Cell 43, 405–413 (1985). doi: 10.1016/0092-8674(85)90170-9 [PubMed: 3907856]
26. Hou M, Xu D, Björkholm M, Gruber A, Real-time quantitative telomeric repeat amplification protocol assay for the detection of telomerase activity. Clin. Chem 47, 519–524 (2001). [PubMed: 11238306]
27. Cucinotta FA, Space radiation risks for astronauts on multiple International Space Station missions. PLOS ONE 9, e96099 (2014). doi: 10.1371/journal.pone.0096099 [PubMed: 24759903]
28. George K, Rhone J, Beitman A, Cucinotta FA, Cytogenetic damage in the blood lymphocytes of astronauts: Effects of repeat long-duration space missions. Mutat. Res 756, 165–169 (2013). doi: 10.1016/j.mrgentox.2013.04.007 [PubMed: 23639573]
29. Ray FA et al., Directional genomic hybridization for chromosomal inversion discovery and detection. Chromosome Res. 21, 165–174 (2013). doi: 10.1007/s10577-013-9345-0 [PubMed: 23572395]
30. Ray FA et al., Directional genomic hybridization: Inversions as a potential biodosimeter for retrospective radiation exposure. Radiat. Environ. Biophys 53, 255–263 (2014). doi: 10.1007/s00411-014-0513-1 [PubMed: 24477407]
31. Cornforth MN, Durante M, Radiation quality and intrachromosomal aberrations: Size matters. Mutat. Res 836 (part A), 28–35 (2018). doi: 10.1016/j.mrgentox.2018.05.002
32. George K, Chappell LJ, Cucinotta FA, Persistence of space radiation induced cytogenetic damage in the blood lymphocytes of astronauts. Mutat. Res 701, 75–79 (2010). doi: 10.1016/j.mrgentox.2010.02.007 [PubMed: 20176126]
33. Jenkinson G, Pujadas E, Goutsias J, Feinberg AP, Potential energy landscapes identify the information-theoretic nature of the epigenome. Nat. Genet 49, 719–729 (2017). doi: 10.1038/ng.3811 [PubMed: 28346445]
34. Koyanagi A, Sekine C, Yagita H, Expression of Notch receptors and ligands on immature and mature T cells. Biochem. Biophys. Res. Commun 418, 799–805 (2012). doi: 10.1016/j.bbrc.2012.01.106 [PubMed: 22310713]
35. Nakaya M et al., Inflammatory T cell responses rely on amino acid transporter ASCT2 facilitation of glutamine uptake and mTORC1 kinase activation. Immunity 40, 692–705 (2014). doi: 10.1016/j.immuni.2014.04.007 [PubMed: 24792914]
36. Thaventhiran JE, Fearon DT, Gattinoni L, Transcriptional regulation of effector and memory $CD8^+$ T cell fates. Curr. Opin. Immunol. 25, 321–328 (2013). doi: 10.1016/j.coi.2013.05.010 [PubMed: 23747000]
37. de Batlle J et al., Association between W3 and W6 fatty acid intakes and serum inflammatory markers in COPD. J. Nutr. Biochem 23, 817–821 (2012). doi: 10.1016/j.jnutbio.2011.04.005 [PubMed: 21889886]
38. Calder PC, Polyunsaturated fatty acids and inflammatory processes: New twists in an old tale. Biochimie 91, 791–795 (2009). doi: 10.1016/j.biochi.2009.01.008 [PubMed: 19455748]
39. Human Microbiome Project Consortium, Structure, function and diversity of the healthy human microbiome. Nature 486, 207–214 (2012). doi: 10.1038/nature11234 [PubMed: 22699609]
40. Li S et al., Multi-platform assessment of transcriptome profiling using RNA-seq in the ABRF next-generation sequencing study. Nat. Biotechnol 32, 915–925 (2014). doi: 10.1038/nbt.2972 [PubMed: 25150835]
41. SEQC/MAQC-III Consortium, A comprehensive assessment of RNA-seq accuracy, reproducibility and information content by the Sequencing Quality Control Consortium. Nat. Biotechnol 32, 903–914 (2014). doi: 10.1038/nbt.2957 [PubMed: 25150838]
42. Gardiner CM, Finlay DK, What fuels natural killers? Metabolism and NK cell responses. Front. Immunol 8, 367 (2017). doi: 10.3389/fimmu.2017.00367 [PubMed: 28421073]

43. Beheshti A, Cekanaviciute E, Smith DJ, Costes SV, Global transcriptomic analysis suggests carbon dioxide as an environmental stressor in spaceflight: A systems biology GeneLab case study. Sci. Rep 8, 4191 (2018). doi: 10.1038/s41598-018-22613-1 [PubMed: 29520055]
44. Norsk P, Asmar A, Damgaard M, Christensen NJ, Fluid shifts, vasodilatation and ambulatory blood pressure reduction during long duration spaceflight. J. Physiol 593, 573–584 (2015). doi: 10.1113/jphysiol.2014.284869 [PubMed: 25774397]
45. Arbeille P, Provost R, Zuj K, Carotid and femoral artery intima-media thickness during 6 months of spaceflight. Aerosp. Med. Hum. Perform 87, 449–453 (2016). doi: 10.3357/AMHP.4493.2016 [PubMed: 27099083]
46. Zwart SR et al., Body mass changes during long-duration spaceflight. Aviat. Space Environ. Med 85, 897–904 (2014). doi: 10.3357/ASEM.3979.2014 [PubMed: 25197887]
47. Smith SM et al., Bone metabolism and renal stone risk during International Space Station missions. Bone 81, 712–720 (2015). doi: 10.1016/j.bone.2015.10.002 [PubMed: 26456109]
48. Smith SM et al., Fifty years of human space travel: Implications for bone and calcium research. Annu. Rev. Nutr 34, 377–400 (2014). doi: 10.1146/annurev-nutr-071813-105440 [PubMed: 24995691]
49. Wang X et al., LRG1 promotes angiogenesis by modulating endothelial TGF-β signalling. Nature 499, 306–311 (2013). doi: 10.1038/nature12345 [PubMed: 23868260]
50. Zwart SR et al., Genotype, B-vitamin status, and androgens affect spaceflight-induced ophthalmic changes. FASEB J. 30, 141–148 (2016). doi: 10.1096/fj.15-278457 [PubMed: 26316272]
51. Zwart SR et al., Vision changes after spaceflight are related to alterations in folate- and vitamin B-12-dependent one-carbon metabolism. J. Nutr 142, 427–431 (2012). doi: 10.3945/jn.111.154245 [PubMed: 22298570]
52. Basner M et al., Development and validation of the cognition test battery for spaceflight. Aerosp. Med. Hum. Perform 86, 942–952 (2015). doi: 10.3357/AMHP.4343.2015 [PubMed: 26564759]
53. Zhao Y et al., A mutational analysis of Caenorhabditis elegans in space. Mutat. Res 601, 19–29 (2006). doi: 10.1016/j.mrfmmm.2006.05.001 [PubMed: 16765996]
54. Shammas MA, Telomeres, lifestyle, cancer, and aging. Curr. Opin. Clin. Nutr. Metab. Care 14, 28–34 (2011). doi: 10.1097/MCO.0b013e32834121b1 [PubMed: 21102320]
55. Pendergrass WR, Penn PE, Li J, Wolf NS, Age-related telomere shortening occurs in lens epithelium from old rats and is slowed by caloric restriction. Exp. Eye Res 73, 221–228 (2001). doi: 10.1006/exer.2001.1033 [PubMed: 11446772]
56. Laimer M et al., Telomere length increase after weight loss induced by bariatric surgery: Results from a 10 year prospective study. Int. J. Obes 40, 773–778 (2016). doi: 10.1038/ijo.2015.238
57. Cherkas LF et al., The association between physical activity in leisure time and leukocyte telomere length. Arch. Intern. Med 168, 154–158 (2008). doi: 10.1001/archinternmed.2007.39 [PubMed: 18227361]
58. Carulli L et al., Telomere length elongation after weight loss intervention in obese adults. Mol. Genet. Metab 118, 138–142 (2016). doi: 10.1016/j.ymgme.2016.04.003 [PubMed: 27157420]
59. Boccardi V, Paolisso G, Mecocci P, Nutrition and lifestyle in healthy aging: The telomerase challenge. Aging 8, 12–15 (2016). doi: 10.18632/aging.100886 [PubMed: 26826704]
60. Arsenis NC, You T, Ogawa EF, Tinsley GM, Zuo L, Physical activity and telomere length: Impact of aging and potential mechanisms of action. Oncotarget 8, 45008–45019 (2017). doi: 10.18632/oncotarget.16726 [PubMed: 28410238]
61. Turroni S et al., Temporal dynamics of the gut microbiota in people sharing a confined environment, a 520-day ground-based space simulation, MARS500. Microbiome 5, 39 (2017). doi: 10.1186/s40168-017-0256-8 [PubMed: 28340597]
62. Mardanov AV et al., Metagenomic analysis of the dynamic changes in the gut microbiome of the participants of the MARS-500 experiment, simulating long term space flight. Acta Naturae 5, 116–125 (2013). [PubMed: 24303207]
63. Mienaltowski MJ, Birk DE, Structure, physiology, and biochemistry of collagens. Adv. Exp. Med. Biol 802, 5–29 (2014). doi: 10.1007/978-94-007-7893-1_2 [PubMed: 24443018]
64. Sasaki S, Aquaporin 2: From its discovery to molecular structure and medical implications. Mol. Aspects Med 33, 535–546 (2012). doi: 10.1016/j.mam.2012.03.004 [PubMed: 23078817]

65. Yamada H, Chen D, Monstein HJ, Håkanson R, Effects of fasting on the expression of gastrin, cholecystokinin, and somatostatin genes and of various housekeeping genes in the pancreas and upper digestive tract of rats. Biochem. Biophys. Res. Commun 231, 835–838 (1997). doi: 10.1006/bbrc.1997.6198 [PubMed: 9070905]
66. Nguyen Dinh Cat A, Touyz RM, A new look at the renin-angiotensin system—Focusing on the vascular system. Peptides 32, 2141–2150 (2011). doi: 10.1016/j.peptides.2011.09.010 [PubMed: 21945916]
67. Michel FS et al., Urinary angiotensinogen excretion is associated with blood pressure independent of the circulating renin-angiotensin system in a group of African ancestry. Hypertension 64, 149–156 (2014). doi: 10.1161/HYPERTENSIONAHA.114.03336 [PubMed: 24777983]
68. Zhang J et al., Ageing and the telomere connection: An intimate relationship with inflammation. Ageing Res. Rev 25, 55–69 (2016). doi: 10.1016/j.arr.2015.11.006 [PubMed: 26616852]
69. Stone RC et al., Telomere length and the cancer-atherosclerosis trade-off. PLOS Genet. 12, e1006144 (2016). doi: 10.1371/journal.pgen.1006144 [PubMed: 27386863]
70. Crucian BE et al., Immune system dysregulation during spaceflight: Potential countermeasures for deep space exploration missions. Front. Immunol 9, 1437 (2018). doi: 10.3389/fimmu.2018.01437 [PubMed: 30018614]
71. Mader TH et al., Optic disc edema in an astronaut after repeat long-duration space flight. J. Neuroophthalmol 33, 249–255 (2013). doi: 10.1097/WNO.0b013e31829b41a6 [PubMed: 23851997]
72. Zwart SR et al., Astronaut ophthalmic syndrome. FASEB J. 31, 3746–3756 (2017). doi: 10.1096/fj.201700294 [PubMed: 28546443]
73. Arbeille P, Provost R, Zuj K, Vincent N, Measurements of jugular, portal, femoral, and calf vein cross-sectional area for the assessment of venous blood redistribution with long duration spaceflight (Vessel Imaging Experiment). Eur. J. Appl. Physiol 115, 2099–2106 (2015). doi: 10.1007/s00421-015-3189-6 [PubMed: 25991027]
74. Hughson RL et al., Increased postflight carotid artery stiffness and inflight insulin resistance resulting from 6-mo spaceflight in male and female astronauts. Am. J. Physiol. Heart Circ. Physiol 310, H628–H638 (2016). doi: 10.1152/ajpheart.00802.2015 [PubMed: 26747504]
75. Lorenz MW, Markus HS, Bots ML, Rosvall M, Sitzer M, Prediction of clinical cardiovascular events with carotid intima-media thickness: A systematic review and meta-analysis. Circulation 115, 459–467 (2007). doi: 10.1161/CIRCULATIONAHA.106.628875 [PubMed: 17242284]
76. Walldius G, Jungner I, The apoB/apoA-I ratio: A strong, new risk factor for cardiovascular disease and a target for lipid-lowering therapy—a review of the evidence. J. Intern. Med 259, 493–519 (2006). doi: 10.1111/j.1365-2796.2006.01643.x [PubMed: 16629855]
77. Florvall G, Basu S, Larsson A, Apolipoprotein A1 is a stronger prognostic marker than are HDL and LDL cholesterol for cardiovascular disease and mortality in elderly men. J. Gerontol. A Biol. Sci. Med. Sci 61, 1262–1266 (2006). doi: 10.1093/gerona/61.12.1262 [PubMed: 17234819]
78. Benn M, Nordestgaard BG, Jensen GB, Tybjaerg-Hansen A, Improving prediction of ischemic cardiovascular disease in the general population using apolipoprotein B: The Copenhagen City Heart Study. Arterioscler. Thromb. Vasc. Biol 27, 661–670 (2007). doi: 10.1161/01.ATV.0000255580.73689.8e [PubMed: 17170368]
79. Ade CJ, Broxterman RM, Charvat JM, Barstow TJ, Incidence rate of cardiovascular disease end points in the National Aeronautics and Space Administration Astronaut Corps. J. Am. Heart Assoc 6, e005564 (2017). doi: 10.1161/JAHA.117.005564 [PubMed: 28784652]
80. Reynolds RJ, Day SM, Mortality among U.S. astronauts: 1980–2009. Aviat. Space Environ. Med 81, 1024–1027 (2010). doi: 10.3357/ASEM.2847.2010 [PubMed: 21043299]
81. Mulavara AP et al., Physiological and functional alterations after spaceflight and bed rest. Med. Sci. Sports Exerc 50, 1961–1980 (2018). doi: 10.1249/MSS.0000000000001615 [PubMed: 29620686]
82. Behjati S et al., Mutational signatures of ionizing radiation in second malignancies. Nat. Commun 7, 12605 (2016). doi: 10.1038/ncomms12605 [PubMed: 27615322]

83. Berardinelli F et al., The role of telomere length modulation in delayed chromosome instability induced by ionizing radiation in human primary fibroblasts. Environ. Mol. Mutagen 54, 172–179 (2013). doi: 10.1002/em.21761 [PubMed: 23401031]

84. Cucinotta FA, Hamada N, Little MP, No evidence for an increase in circulatory disease mortality in astronauts following space radiation exposures. Life Sci. Space Res 10, 53–56 (2016). doi: 10.1016/j.lssr.2016.08.002

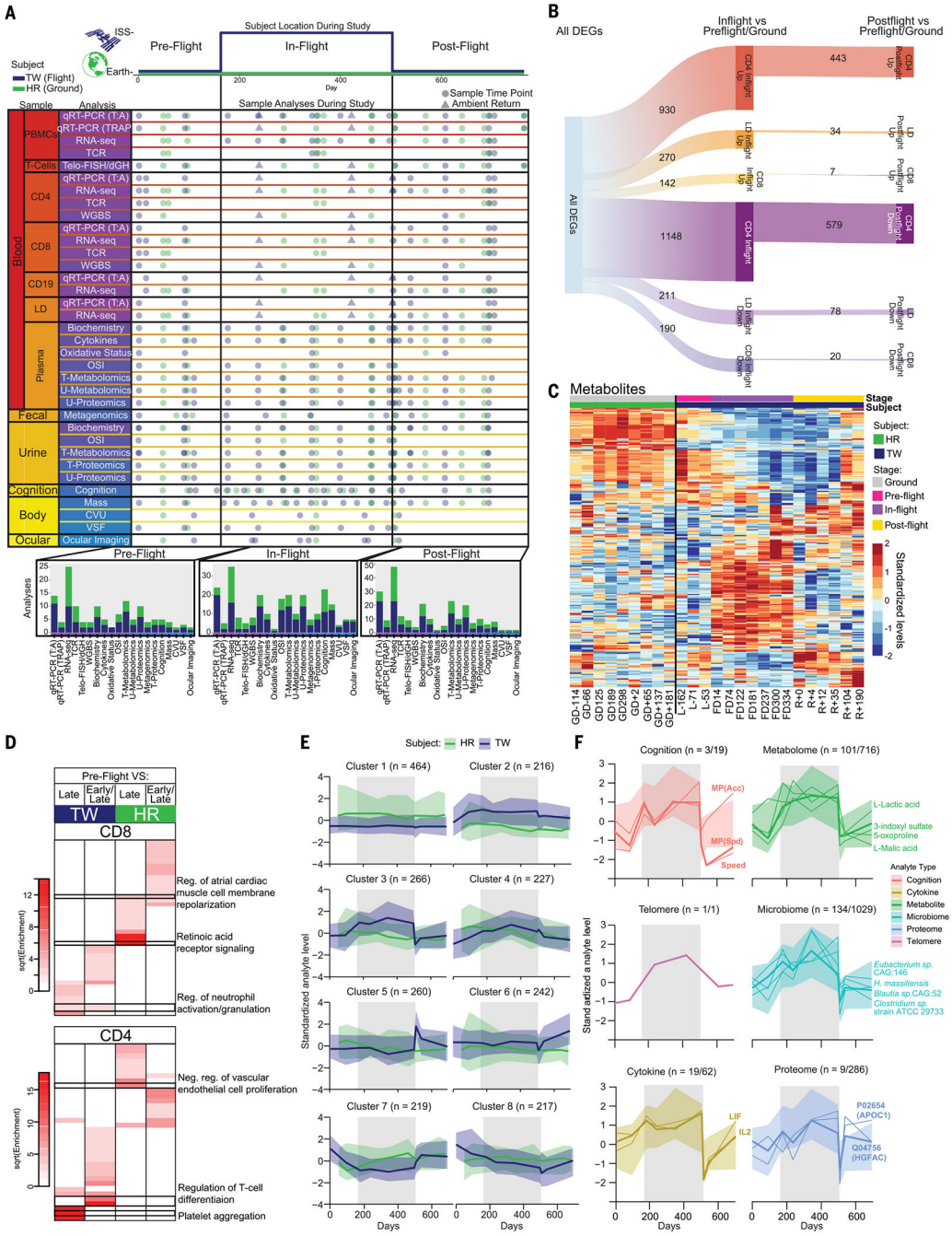

Fig. 1. Study design and human spaceflight metrics.

The flight subject (TW, blue) and his identical twin (HR, green) were each studied over 25 months using a comprehensive set of health and biological metrics. (**A**) Earth-based and spaceflight collections include blood, sorted cells (CD4, CD8, CD19, and LD), stool, buccal, saliva, urine, and AR blood. TCR, T cell receptor sequencing; T- and U-Metabolomics, targeted and untargeted metabolomics; OSI, oxidative stress and inflammation; T- and U-Proteomics, targeted and untargeted proteomics; CVU, cardiac and vascular ultrasound; VSF, vascular structure and function. (**B**) Gene expression changes in TW inflight and

postflight compared with the preflight period. All time points of HR were used to account for normal levels of variance and noise in gene expression. Genes that were significantly altered inflight after controlling for subject baselines and AR effect are reported. Gene expression changes were reported for any gene with $q < 0.05$ in a multivariate model that utilized expression values for polyadenylated [poly $(A)^+$] and ribosomal RNA depleted transcripts. (**C**) Metabolites present at significantly different levels in HR and TW or between pre-, in-, and postflight periods. Heatmap represents median-normalized $\log_2$ intensity for each analyte, scaled across all samples. Red color indicates relative enrichment, whereas blue indicates relative depletion. (**D**) GO analysis of genes ranked on the basis of epigenetic discordance at their promoters. Comparisons of preflight samples to inflight (early and late, and combined early and late) and postflight samples are shown for both CD4 and CD8 cells. Heatmaps represent transformed enrichment values [square root (sqrt) of enrichment] for GO categories with a raw enrichment value >5. Reg., regulation; neg. reg., negative regulation. (**E**) *C*-means clustering of multiomics data reveals longitudinal patterns associated with spaceflight. Analyte abundance (scaled) plotted over time for the identified clusters from the integrated metabolome, proteome, cytokine, cognition, and microbiome datasets is shown. Median abundance (bold) per cluster and 5th and 95th percentiles of abundance (shaded) are indicated. The gray shaded region indicates the inflight period. *n*, number of analytes in cluster. (**F**) Individual plots of the different analyte types that compose the spaceflight-dependent cluster, cluster 3, from (E). Telomere levels are plotted adjacent to the cluster members for reference. Median abundance (bold) per cluster and 5th and 95th percentiles of abundance (shaded) are indicated. Thin lines show annotated examples of analytes from cluster 3. For Cognition, accuracy [MP(Acc)] and speed [MP(Spd)] on the motor praxis task as well as standardized speed across cognitive domains (speed) are shown. *n*, number of analytes in cluster; CAG, coabundance gene groups.

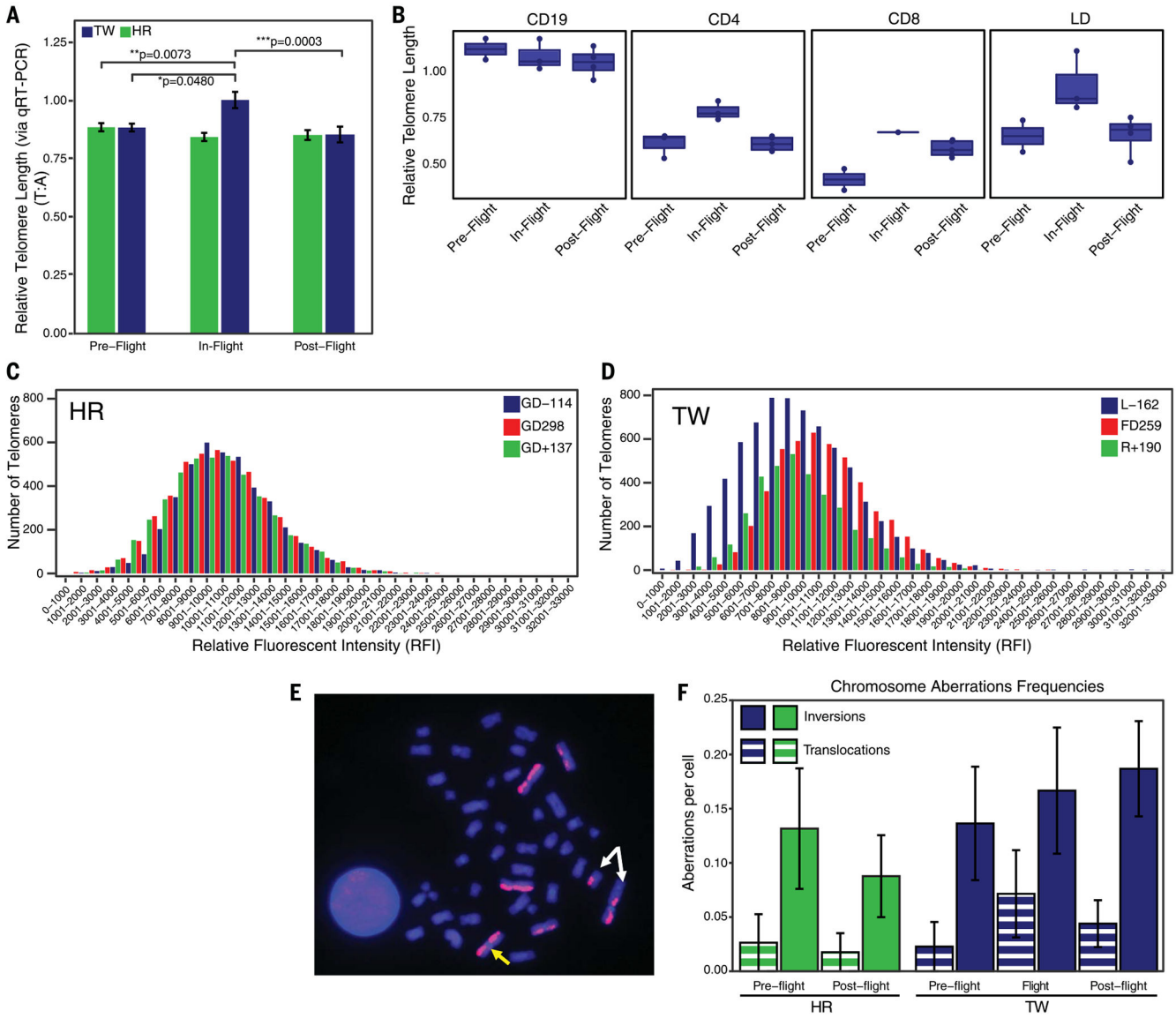

Fig. 2. Telomere length dynamics and DNA damage responses.

(**A**) Relative average telomere length in PBMCs (DNA) pre-, in-, and postflight assessed by qRT-PCR for HR (green) and TW (blue). Significance was tested by one-way ANOVA, and error bars represent SEM. (**B**) Relative average telomere length for TW in sorted PBMC subpopulations, CD19 B cells, CD4 and CD8 T cells, and LD fractions, pre-, in-, and postflight. Boxplot whiskers show min and max. (**C** and **D**) Telo-FISH–generated histograms of individual telomere length distributions [shorter to longer, lower to higher relative fluorescent intensity (RFI)] for HR (C) and TW (D) preflight (blue), inflight (red), and postflight (green). (**E**) Cytogenetic analysis of DNA damage utilizing dGH paints (pink) for chromosomes 1, 2, and 3 facilitated simultaneous detection of translocations and inversions. Representative image of dGH on a metaphase chromosome spread illustrating an intrachromosomal inversion (yellow arrow) and an interchromosomal reciprocal translocation (white arrows). (**F**) Quantification of translocation (striped bars) and inversion

(solid bars) frequencies for HR and TW pre-, in-, and postflight. Results were not statistically significant (one-way ANOVA). Error bars represent SEM.

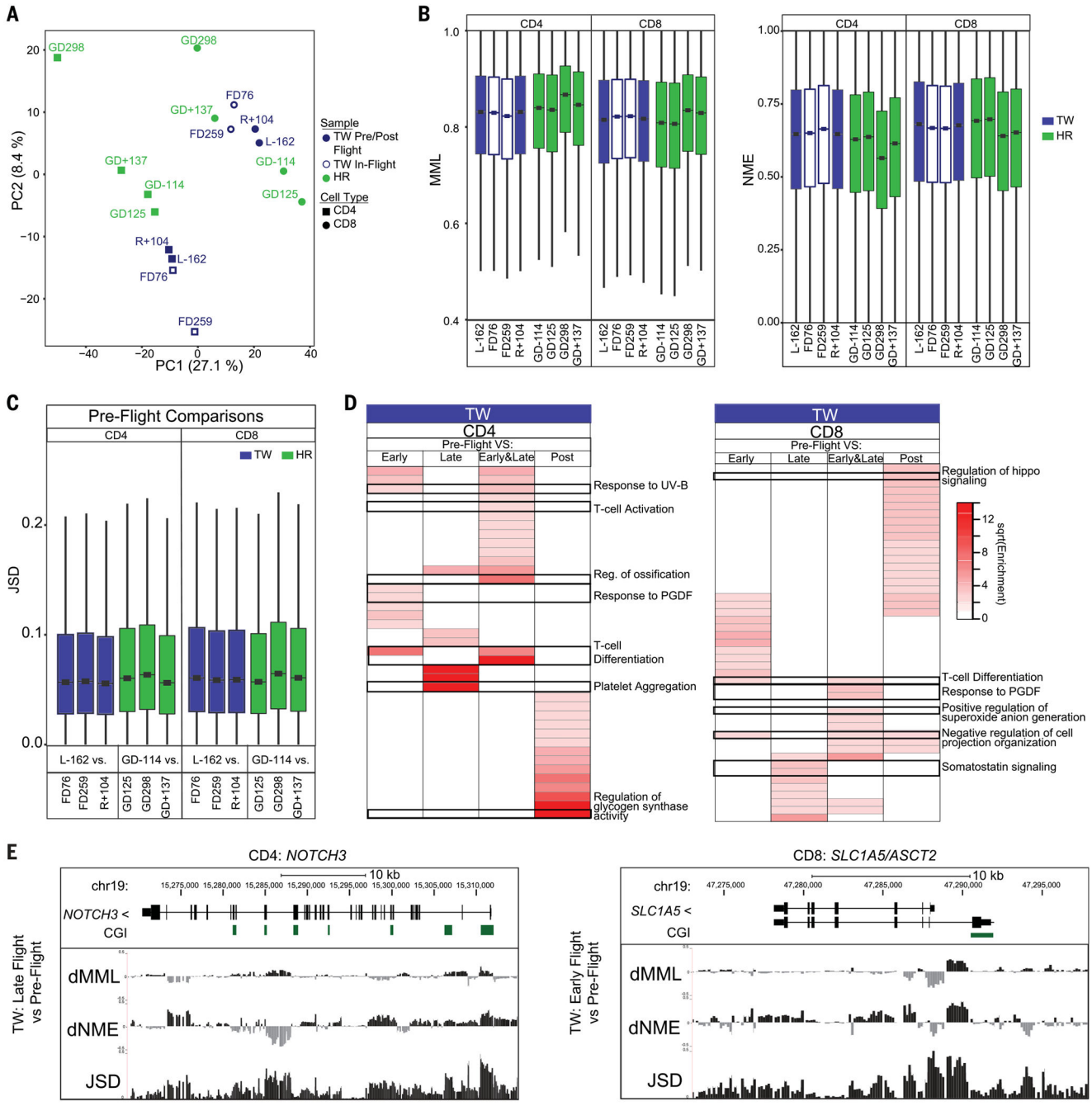

Fig. 3. Global changes in DNA methylation during spaceflight.

(**A**) PCA of distances derived from average CpG methylation levels in 1-kb intervals along the chromosomes in each sample (CD4 and CD8 lymphocytes collected from each subject). (**B**) Genome-wide distributions of MML and NME values in CD4 and CD8 lymphocytes collected from each subject at indicated time points. (**C**) Genome-wide distributions of JSDs within each subject in comparisons of preflight to the indicated inflight and postflight time points in CD4 and CD8 cells. (**D**) Heatmaps representing transformed enrichment values (square root of enrichment) for GO categories with a raw enrichment value >5 in TW for

comparisons of preflight (L–162) samples to inflight (early, FD76; late, FD259) and postflight (R+104) samples in CD4 and CD8 cells. (**E**) University of California, Santa Cruz, Genome Browser images of *NOTCH3* and *SLC1A5* with peaks of JSD at their promoters in TW when comparing inflight (FD259, for *NOTCH3*, and FD76, for *SLC1A5*) to preflight (L–162) samples from CD4 (for *NOTCH3*) and CD8 (for *SLC1A5*) cells. Differential MML (dMML) and differential NME (dNME) values are also plotted, with negative values indicating reduced MML or NME at the inflight time points compared with preflight time points. For all boxplots, center lines indicate median, boxes indicate interquartile range (IQR), and whiskers indicate 1.5 × IQR. CGI, CpG island; chr. 19, chromosome 19.

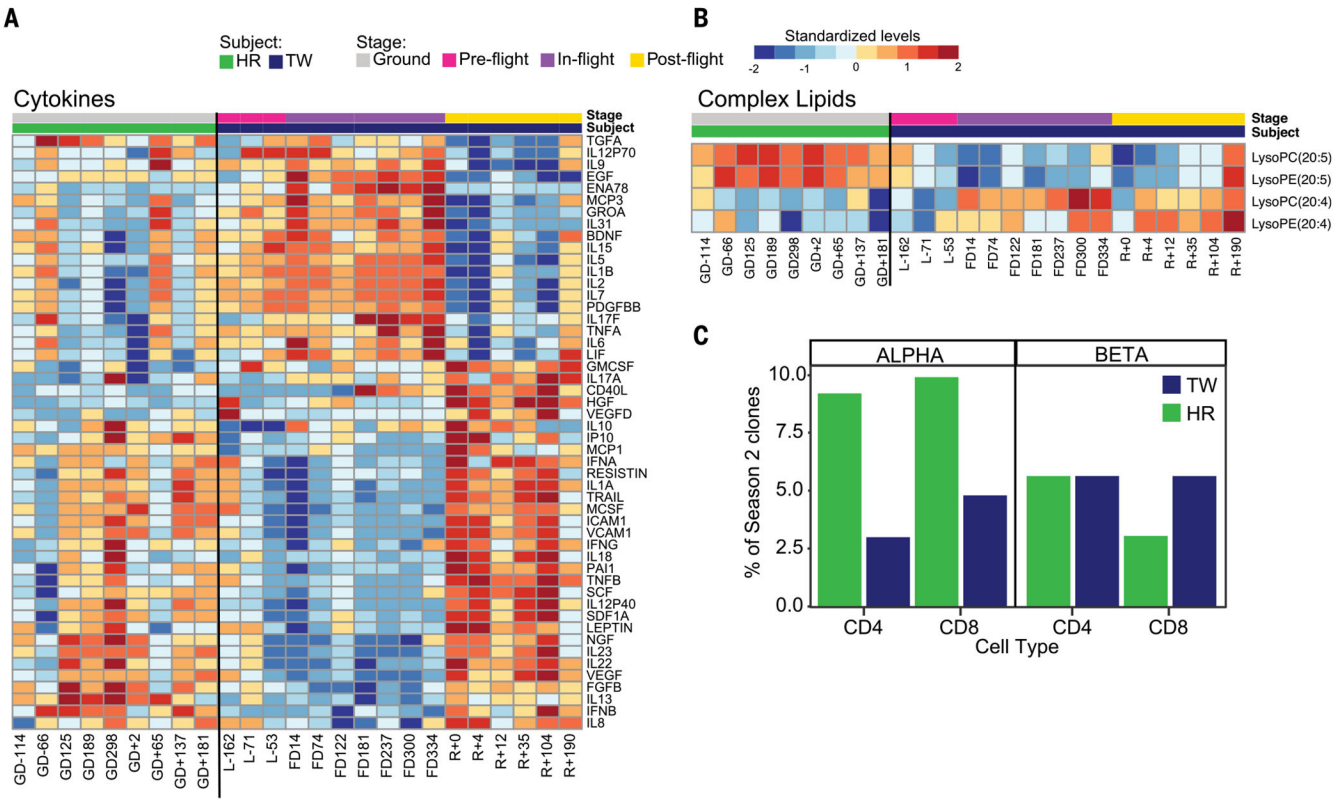

Fig. 4. Lipids and vaccine response.

(**A**) Cytokines present at significantly different levels in HR and TW or between pre-, in-, and postflight periods. Heatmap represents median-normalized $\log_2$ intensity for each analyte, scaled across all samples. Red color indicates relative enrichment, whereas blue indicates relative depletion. (**B**) Relative levels (median-normalized, scaled $\log_2$ intensity) of complex lipids containing ω-3 and ω-6 fatty acids in HR and TW, from untargeted plasma metabolomics. Red color indicates relative enrichment, whereas blue indicates relative depletion. LysoPC, lysophosphatidylcholine; LysoPE, lysophosphatidylethanolamine. (**C**) Immunological and postvaccination response to spaceflight. For each subject, the proportion of season 2 clones present in the database of influenza vaccination-responsive CDR3 clones derived from year 1 and 3 vaccinations is shown for each cell type and respective TCR chain (FDR < 0.05).

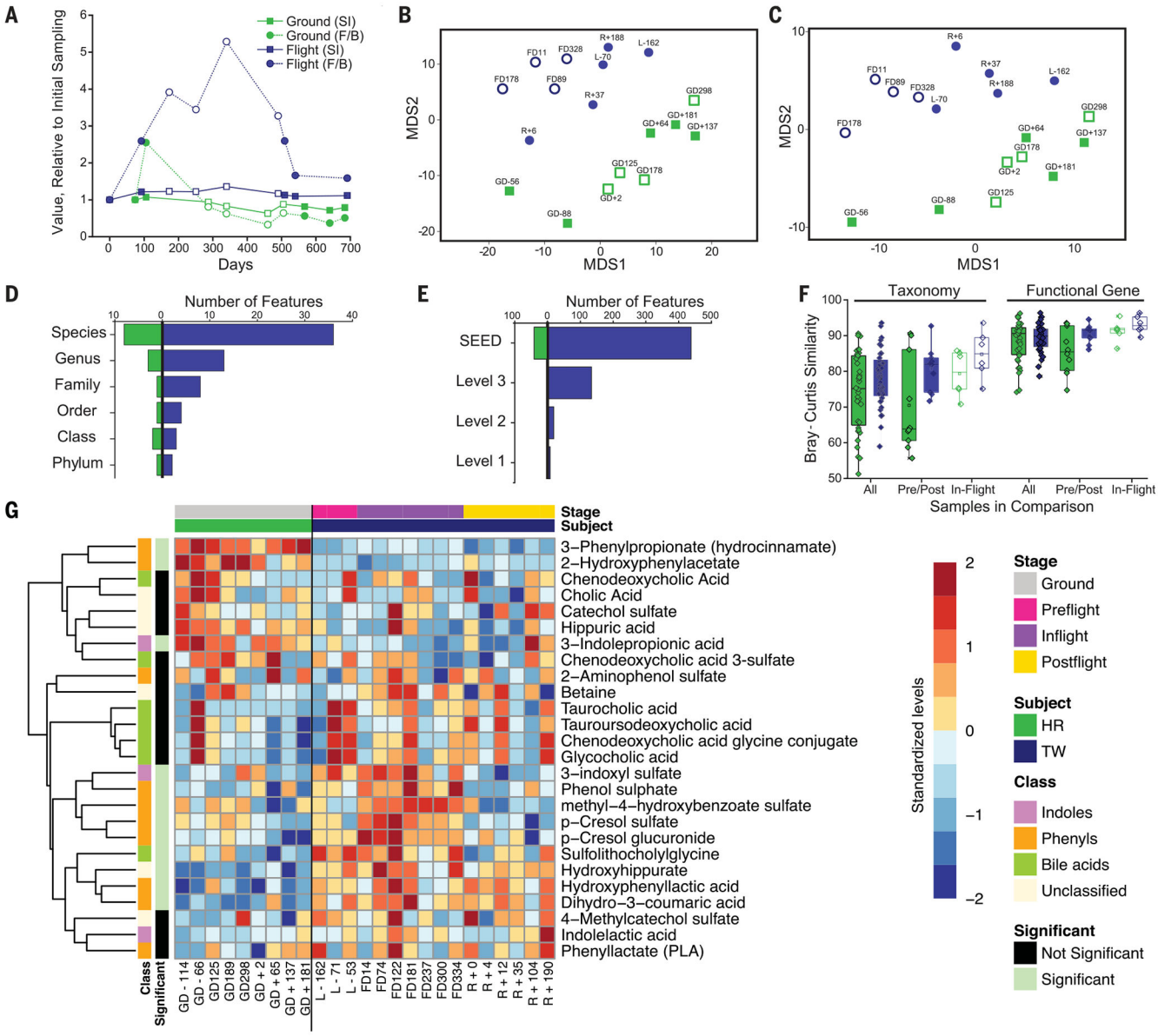

Fig. 5. Effect of spaceflight on the fecal microbial community structure of the flight subject relative to the twin ground subject.

Samples are color coded by subject (TW, blue; HR, green), with open symbols representing flight samples from TW or flight-equivalent samples from HR. (**A**) Taxonomic alpha diversity parameters for HR and TW over nine sampling events, normalized to the value of the first sampling event for each subject. Shown are the normalized genus-level $\log_2$ SI values for both subjects and the F/B ratio. SI values at the first sampling event were 4.26 and 3.13 for HR and TW, respectively. F/B ratio values at the first sampling event were 2.18 and 0.87 for HR and TW, respectively. (**B** and **C**) Analysis of microbial community taxonomic structure at the genus level (B) and functional gene content (C) using mMDS of annotated shotgun metagenome sequence data. Data were $\log(x + 1)$ transformed, and a resemblance matrix, from Bray-Curtis dissimilarity, was generated. MDS axes 1 and 2 are plotted; two-

dimensional stress values are 0.19 and 0.13 for taxonomic and functional gene analyses, respectively. Sample names represent dates relative to launch. (**D**) Number of microbial features at each taxonomic level that were differentially abundant between the inflight samples and the combined pre- and postflight samples of TW or between the equivalent sets of samples from HR. (**E**) Number of gene functional features at each level (ranged from SEED, that is, the most specific gene functions, to level 1, that is, the most general categories) that were differentially abundant between the inflight samples and the combined pre- and postflight samples of TW or between the equivalent sets of samples from HR. (**F**) Overall similarity of metagenomic sequence data from sample groups was assessed with Bray-Curtis similarity measurements for untransformed data and presented as boxplots. For each subject, all nine samples are compared and plotted (HR and TW; 36 comparisons), followed by pre- and postflight samples only (HR ground and TW ground; 10 comparisons) and flight samples only (HR flight and TW flight; six comparisons). (**G**) Metabolic products associated with microbial metabolism in humans. The heatmap shows relative levels of microbial metabolites detected in the metabolomics data (median-normalized, scaled, $\log_2$ intensity). Red color indicates relative enrichment, whereas blue indicates relative depletion. Row annotations mark different classes of microbial metabolites, including indoles (violet), phenyls (orange), and bile acids (green). Metabolites that were not significantly altered between HR and TW or between pre-, in-, and postflight periods are marked in black.

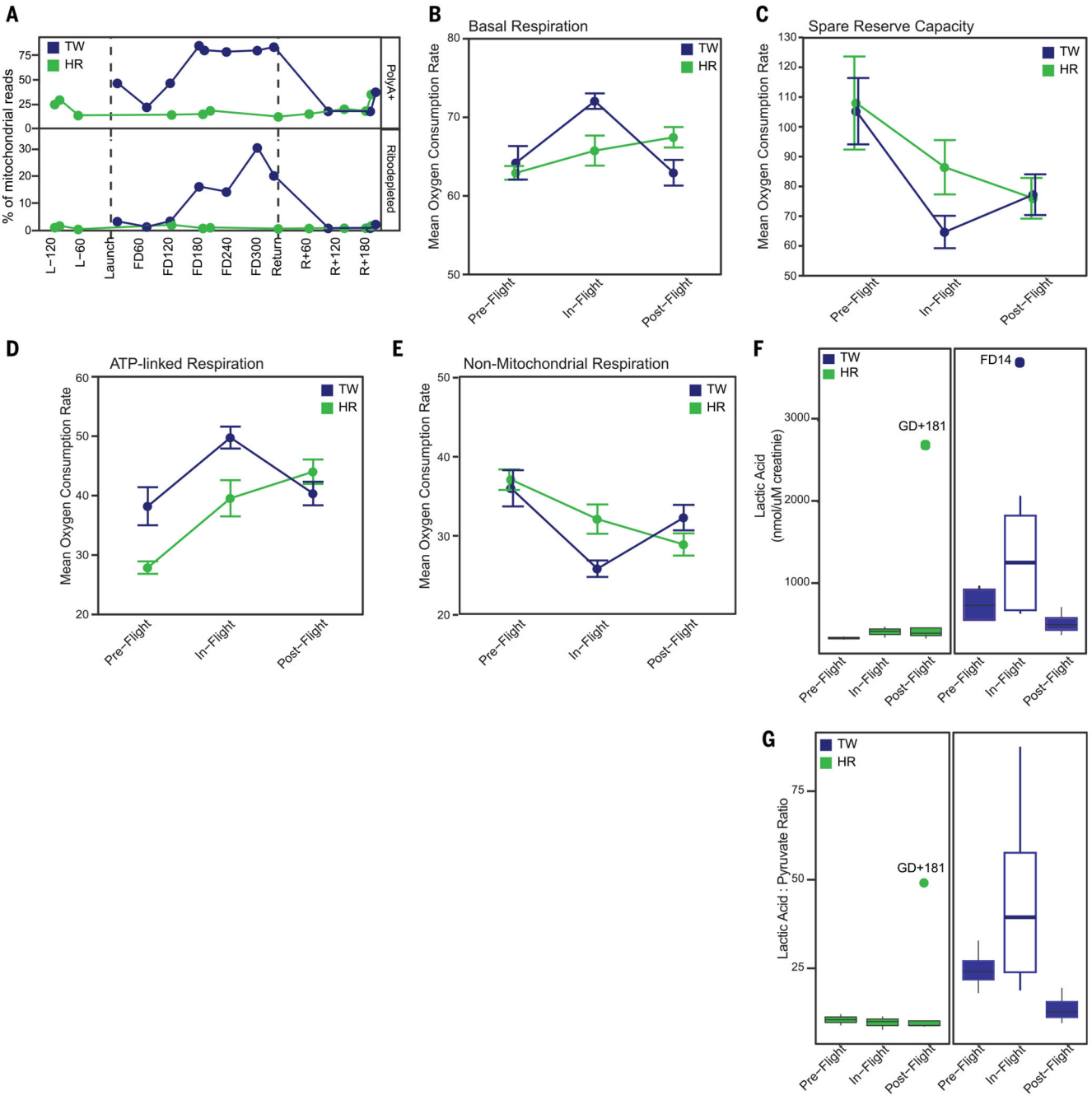

Fig. 6. Mitochondrial functions and Seahorse assays.

(**A**) mtRNA content observed in RNA-seq data for the unsorted frozen PBMC (expressed relative to total number of aligned reads). Sequencing results after library preparation with both poly $(A)^+$ selection and ribosomal depletion. (**B** to **E**) Mean OCR during pre-, in-, and postflight for basal mitochondrial respiration (B), spare reserve capacity (C), ATP-linked respiration (D), and nonmitochondrial respiration (E). L6 muscle cells were treated with plasma from TW and HR collected pre-, in-, and postflight with six to eight assay replicates per time point. OCR was measured before and after the addition of inhibitors (oligomycin, a

complex V inhibitor; FCCP, a protonophore; and antimycin A and rotenone, complex III and I inhibitors, respectively) to derive parameters of mitochondrial respiration. Mean OCR was calculated for each parameter after normalizing for baseline OCR of the L6 cells before the addition of plasma or inhibitors. Error bars represent 95% confidence intervals of the mean OCR of all replicates at each time point for each flight event. (**F**) Boxplots comparing the concentration of lactic acid in urine normalized to urine creatinines (determined by GC-MS targeted metabolomics) pre-, in-, and postflight in TW and HR. (**G**) Boxplots representing the ratio of urine lactic acid to pyruvate pre-, in-, and postflight in TW and HR revealing an inflight shift to anaerobic metabolism in the flight twin.

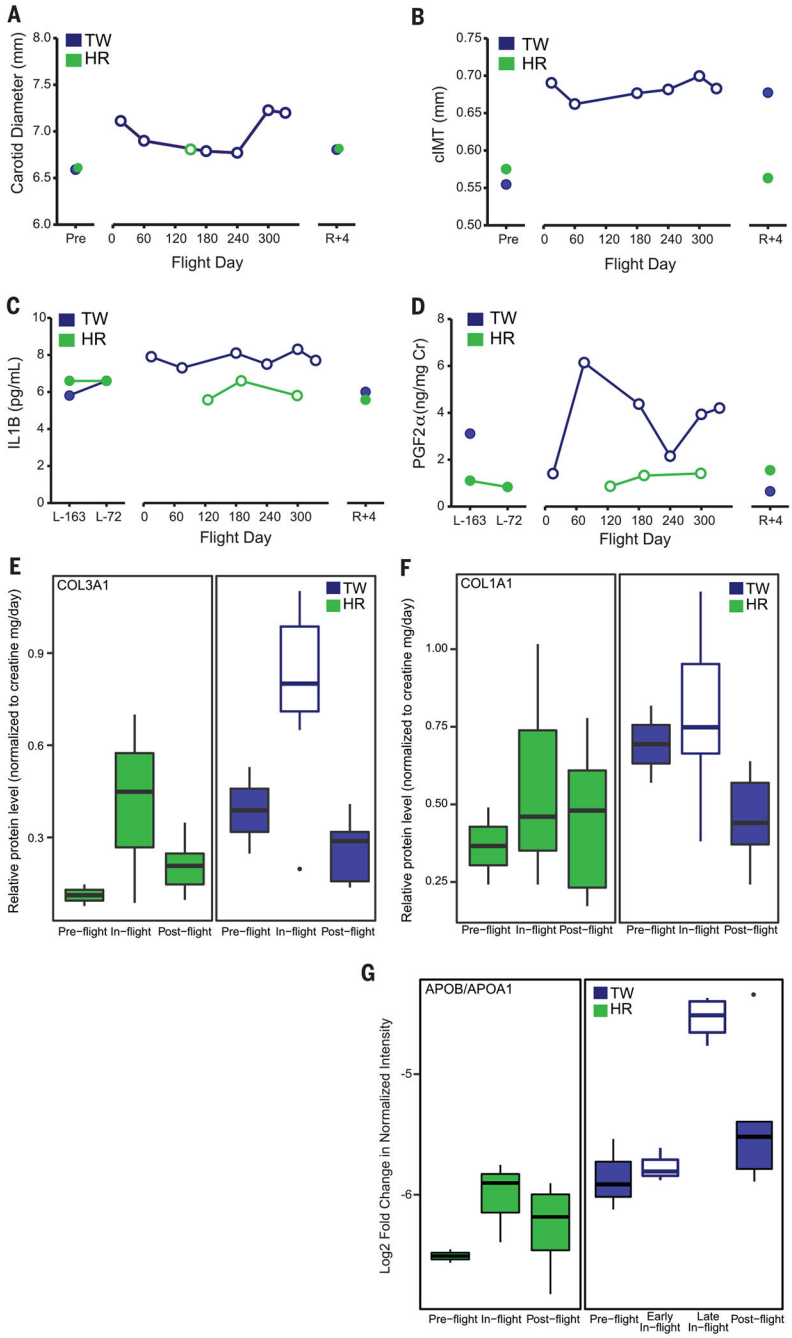

Fig. 7. Vascular adaptations.

(**A** and **B**) Carotid artery diameter during diastole (A) and carotid intima-media thickness (cIMT) (B) measured while supine on the ground and during spaceflight in TW and HR. "Pre" indicates the mean of the two preflight measurements. (**C** and **D**) IL1B (C) and PGF2α (D) as examples of biomarkers of inflammation and oxidative stress that were measured in these two subjects. (**E** and **F**) Boxplots of relative COL3A1 (E) and COL1A1 (F) levels pre-, in-, and postflight for both subjects. (**G**) Ratio of relative plasma levels of

proteins APOB and APOA1 (APOB/APOA1) in both subjects pre-, in-, and postflight, measured using untargeted proteomics (LC-MS).

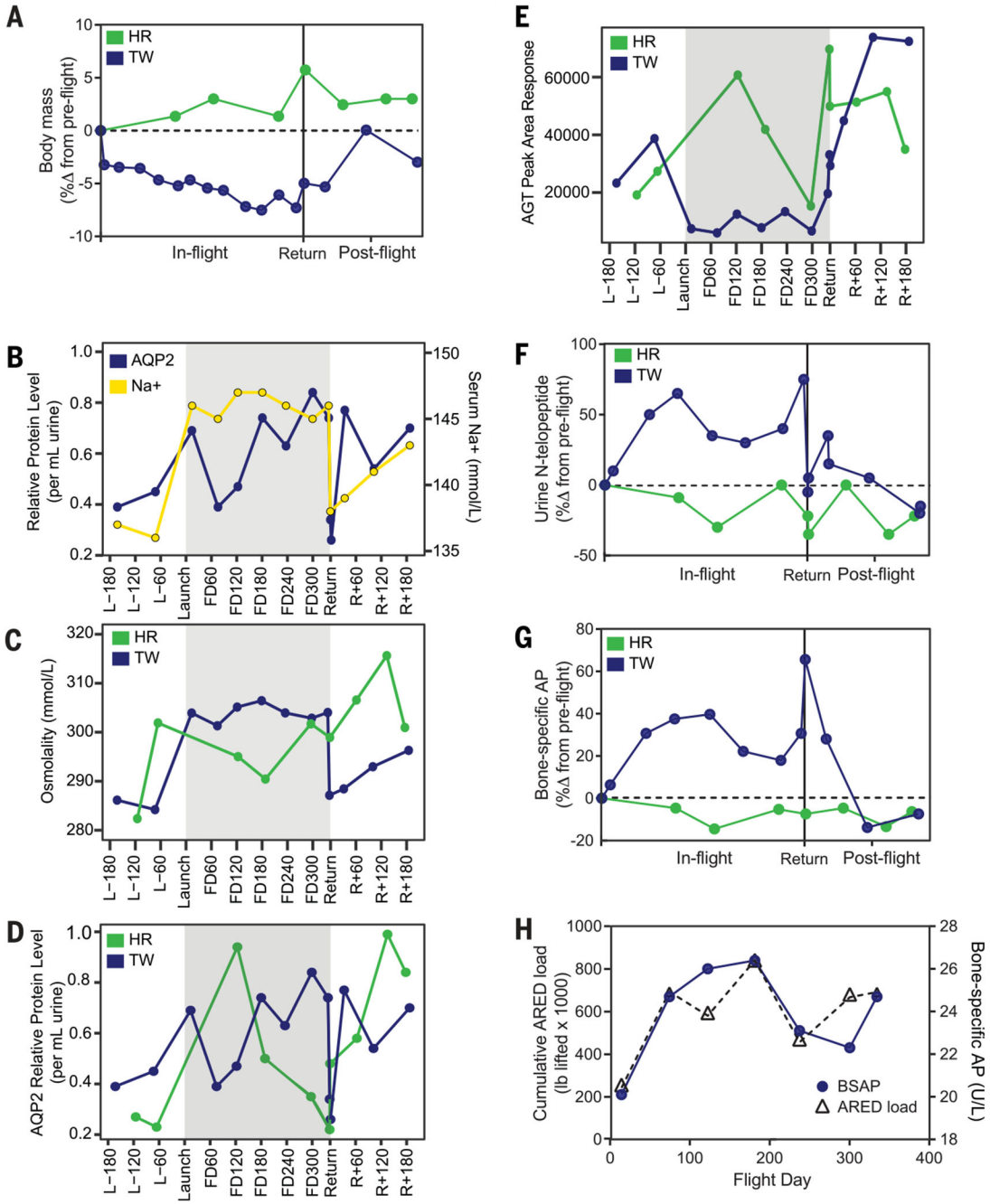

Fig. 8. Body weight, bone formation, fluid regulation, and biochemical activity during spaceflight. Biochemical and biophysical measures during the mission. Data are mean ± SD.

(**A**) Body mass expressed as percent change (Δ) from preflight. (**B**) Relative urine AQP2 concentration in TW (blue circles) plotted along with serum sodium concentrations (yellow circles). (**C**) Calculated plasma osmolality for both subjects. (**D**) Relative urine AQP2 concentrations for both subjects. (**E**) Untargeted (LC-MS) urine proteomics reveals that relative angiotensinogen (AGT) levels inflight correspond with inflight weight loss. In (B) to (E), the shaded area represents inflight time points. (**F** and **G**) Bone breakdown (N-

telopeptide) (F) and bone formation [bone-specific alkaline phosphatase (AP)] (G) markers. Data in (F) and (G) are expressed as percent change from preflight. (**H**) Exercise load using the advanced resistive exercise device (ARED) and bone-specific AP marker. 1 lb = 0.45 kg; U/L, units per liter.

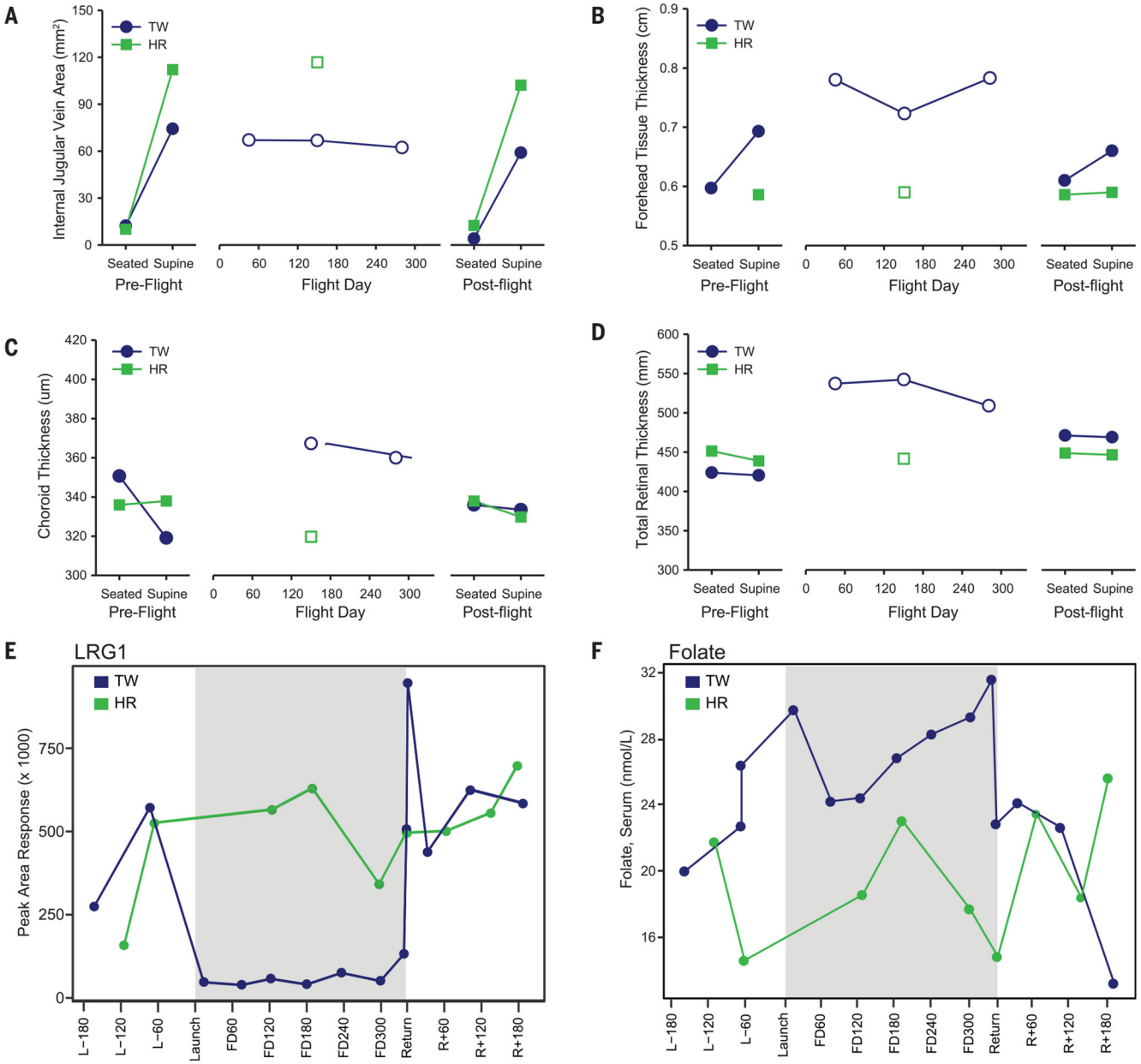

Fig. 9. Fluid shifts and ocular changes.

(**A** and **B**) Internal jugular vein cross-sectional area (A) and forehead skin thickness (B) measured by ultrasound as indicators of acute fluid shifting during the transition from seated to supine during ground-based testing and the chronic fluid shift in weightlessness in TW. (**C** and **D**) Concurrently, ocular measures of choroid thickness (C) and total retinal thickness (D) measured by optical coherence tomography under the same conditions. (**E**) Untargeted proteomics reveals decreased urine excretion of LRG1 in TW during flight relative to ground time points. (**F**) Serum folate is lower in astronauts who experienced ophthalmic issues and was similarly relatively low in both twins. TW's serum folate increased during flight, mirroring the increase in telomere length.

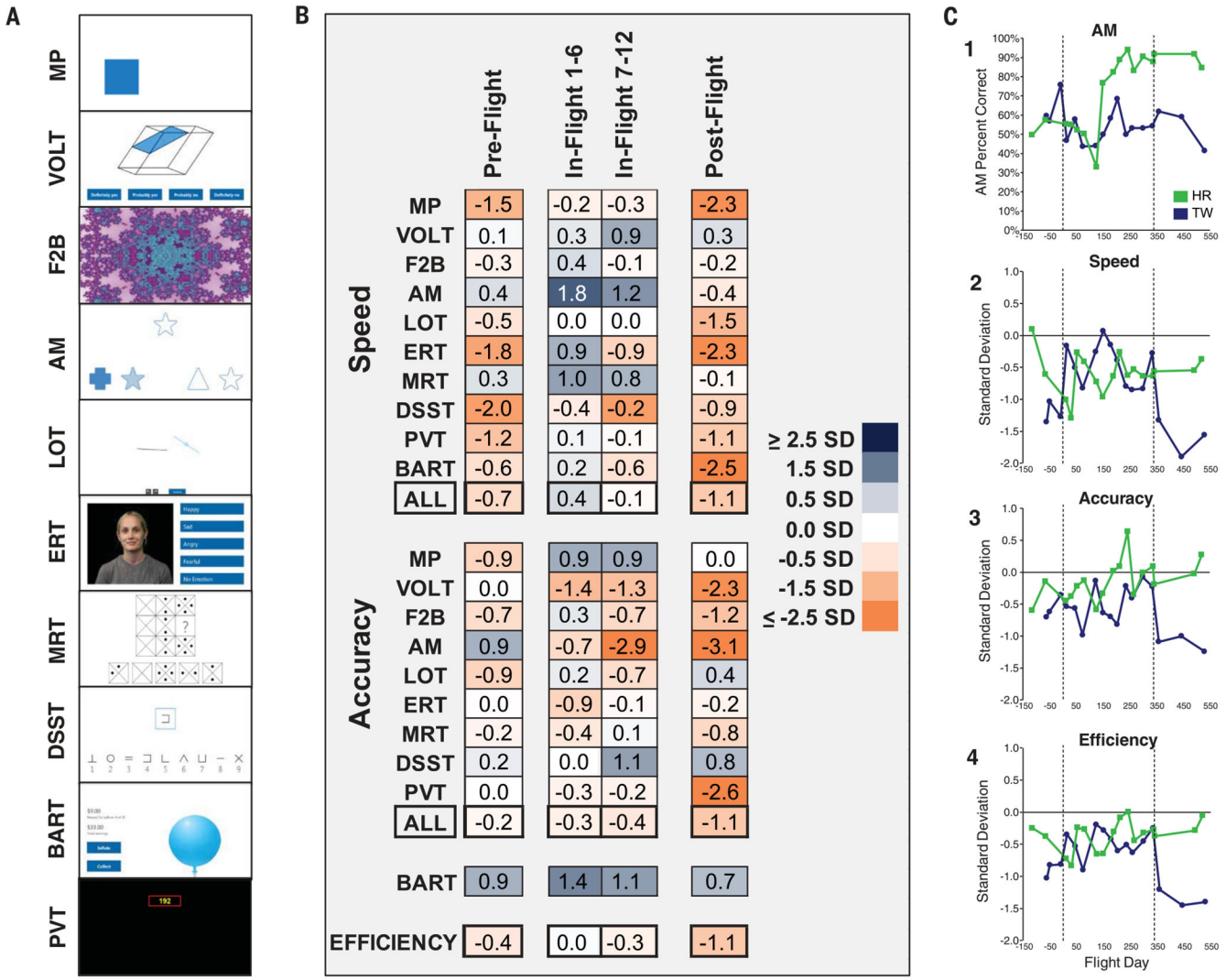

Fig. 10. Cognitive performance results.

(**A**) Representative images of the Cognition battery (10 tasks). MR motor praxis; VOLT, visual object learning test; F2B, fractal 2-back; AM, abstract matching; LOT, line orientation test; ERT, emotion recognition task; MRT, matrix reasoning test; DSST, digit symbol substitution task; BART, balloon analog risk test; RVT, psychomotor vigilance test. (**B**) Heatmap of cognitive performance scores of TW relative to HR during preflight ($N = 3$ tests), the first 6 months inflight (inflight 1 to 6, $N = 6$ tests), the second 6 months inflight (inflight 7 to 12, $N = 5$ tests), and postflight ($N = 3$ tests). Test scores were corrected for practice and stimulus set-difficulty effects. All data were then standardized relative to preflight ground data of 15 astronauts (including TW and HR).Test scores in the heatmap reflect TW scores minus HR scores expressed in SD units. The BART reflects risk-taking behavior and was thus not included in the accuracy score across cognitive domains (accuracy, ALL). Efficiency was calculated as the average of the speed score across cognitive domains (speed, ALL) and the accuracy score across cognitive domains (accuracy, ALL). (**C**) Standardized cognition performance scores for individual test bouts for the AM

test (1) and speed (2), accuracy (3), and efficiency (4) across cognitive domains. The vertical lines indicate launch and landing dates for TW. The AM plot shows that HR (green) had a major insight mid-mission relative to the rules that govern the AM that TW (blue) did not have (50% is performance at chance level on the AM). The speed, accuracy, and efficiency plots demonstrate that the nature of the postflight decline in TW's performance was protracted.

Table 1.

Spaceflight experience of study subjects.

Summary of spaceflight missions (launch and landing dates) as well as durations for study subjects TW and HR.

Subject	Vehicle	Mission	Launch date	Landing date	Duration (days)
TW	Space shuttle	STS-103	12/19/99	12/27/9 9	8
	Space shuttle	STS-118	8/8/07	8/21/07	12.7
	International Space Station	Expedition 25/26	10/7/10	3/16/11	159
	International Space Station	Expedition 43/44/45/46	3/27/15	3/1/16	340
HR	Space shuttle	STS-108	12/5/01	12/17/01	11.8
	Space shuttle	STS-121	7/4/06	7/17/06	12.8
	Space shuttle	STS-124	5/31/14	6/14/14	13.8
	Space shuttle	STS-134	5/16/11	6/1/11	15.7